Single-nucleus resolution mapping of the adult *C. elegans* and its application to elucidate inter- and trans-generational response to alcohol.

Lisa Truong[1,2], Yen-Wei Chen[1,3], Rio Barrere-Cain[4], Karissa Shuck[4], Wen Xiao[5], Max T. Levenson[3], Eduardo da Veiga Beltrame[6], Blake Panter[4], Ella Reich[4], Paul W. Sternberg[6], Xia Yang[7], Patrick Allard[3,4, 8]*

1. Authors contributed equally to the work
2. Human Genetics Graduate Program, UCLA, Los Angeles, CA. 90095.
3. Molecular Toxicology Inter-Departmental Program, UCLA, Los Angeles, CA. 90095.
4. Institute for Society & Genetics, UCLA, Los Angeles, CA. 90095.
5. Department of Microbiology, Immunology, and Molecular Genetics, UCLA, Los Angeles, CA. 90095.
6. Biology and Biological Engineering, California Institute of Technology, Pasadena, CA. 91125.
7. Integrative Biology and Physiology Department, UCLA, Los Angeles, CA. 90095.
8. Molecular Biology Institute, UCLA, Los Angeles, CA. 90095.

* Corresponding Author

Email: pallard@ucla.edu
https://orcid.org/0000-0001-7765-1547

Keywords
C. elegans, snRNA-seq, ethanol, alcohol

Author Contributions

LT, RBC, KS, WX, MTL, BP, and EL performed biological experiments and corresponding analyses, YWC performed bioinformatic analyses, PA and XY supervised experiments, PA and XY supervised analyses, EB devised a visualization approach that assisted cell type assignment and cluster identification which PS supervised, LT, RBC, YWC, XY, and PA wrote the manuscript.

ABSTRACT

Single-cell RNA transcriptomic platforms have significantly contributed to our understanding of tissue heterogeneity as well as of developmental and cellular differentiation trajectories. They also provide an opportunity to map an organism's response to environmental cues with high resolution and unbiasedly identify the cell types that are the most transcriptionally sensitive to exposures. Here, we applied single nucleus RNA-seq experimental and computational approaches to *C. elegans* to establish the transcriptome of the adult nematode and comprehensively characterize the transcriptional impact of ethanol as a model environmental exposure on the entire organism at cell type-resolution over several generations. Clustering, tissue and phenotype enrichment, and gene ontology analyses identified 31 clusters representing a diverse number of adult cell types, including those from syncytial and multi-nucleated tissues which are difficult to assess by single cell RNA-seq, such as the mitotic and meiotic germline, hypodermal cells, and the intestine. We applied this method to identify the impact of inter- and trans-generational exposure to two human-relevant doses of alcohol. Cell type proportions were not significantly altered by ethanol. However, Euclidean distance analysis identified several germline, striated muscle, and neuronal clusters as being major transcriptional targets of ethanol at both the F1 and F3 generations although the relative order of clusters changed between generations. The impact on germline clusters was further confirmed by phenotypic enrichment analysis as well as functional validation, namely a remarkable inter- and trans- generational increase in germline apoptosis, aneuploidy, and embryonic lethality. Together, snRNA-seq of the adult *C. elegans* represents a powerful approach for the detailed examination

of an adult organism's response to environmental cues.

INTRODUCTION

In mammals, *in utero* exposure to alcohol is associated with an array of well-characterized morphological, neurological, and reproductive deficits in the F1 progeny that are grouped into symptoms of Fetal Alcohol Syndrome Disorders (FASD) [1]. The plurality of the conditions associated with FASD reflects the variety of organ systems and processes showing structural and functional anomalies following prenatal alcohol exposure, such as the reproductive system, the central nervous system, craniofacial morphogenesis, the heart, kidney, liver, and gastrointestinal system (reviewed in [2,3]). However, while *in utero* alcohol exposure clearly impacts the function of multiple organ systems, a comprehensive assessment of all organs, tissues, and cell types that are the most affected by alcohol remains lacking [4].

In addition to impacting the health of the F1 progeny, mounting evidence in various model systems, such as mice, rats, *Drosophila*, and *C. elegans*, indicates that at least some exposure-related adverse reproductive and neurobehavioral features also extend beyond the F1 and are detectable in F3 progeny [5–8]. For instance, a rat model of late gestational ethanol exposure demonstrated that not only F1 but also F2 and F3 individuals show an average 50% increase in ethanol intake [9]. Moreover, preconception exposure is sufficient to cause increased alcohol intake in the offspring, together with signs of spatial learning and memory deficits [10]. Notably, the impact of ethanol on alcohol and substance use across several generations is observed in the broader context of several established multi- and transgenerational models in which

various cognitive, behavioral, or physical endpoints are altered (reviewed in [11,12]).

C. elegans is a simplified but highly advantageous model for studying the effects of alcohol and is the most used invertebrate species for modeling FASD (reviewed in [13]). Direct exposure to ethanol causes a variety of dose- and duration-dependent outcomes similar to those elicited in mammals such as growth and fertility impairments, neuro-depressive effects, increase alcohol preference and disinhibition, withdrawal, all supported by the involvement of similar cellular and neurological pathways [14–18]. The *C. elegans* genome is also equipped with the conserved gene families of alcohol and aldehyde dehydrogenases that provide the main metabolic activity towards ethanol which is first processed into acetaldehyde and subsequently into acetate [19]. Finally, its reproductive system, with two gonads opening into a common uterus where embryos initiate their development, provides a window for *in utero* exposure to alcohol.

Recently, the combination of single-cell RNA sequencing (scRNA-seq) technologies and the tractability of the model organism *C. elegans*, with its well-established differentiation lineages and timing, has enabled the layering of transcriptional data with developmental events at both embryonic and larval (L2) stages, as well as the mapping of the entire nervous system [20–22]. This has led, for example, to the identification of gene expression changes that track the development of 502 preterminal and terminal cell types in embryos [21] and the characterization of 27 distinct cell types at larval stages [20]. Furthermore, we and others have shown that *C. elegans* is also a powerful model for the study of multi- and trans- generational responses to environmental stimuli [23–28]. However, single cell transcriptomic approaches have yet to be applied to the characterization of environmental exposures,

including alcohol, at the whole organism level and across generations.

Here, we used RNA-seq from single nuclei to maximize the isolation of diverse cell types, including from the approximately 30% of all somatic cells that are polyploid and from the mostly syncytial adult germline. We applied this approach to examine the transcriptional impact of parental (P0) exposure to two physiologically relevant doses of ethanol on the F1 offspring (inter-generational exposure) as well as on the F3 generation (trans-generational exposure). We show that single nucleus RNA-seq (snRNA-seq) identifies a large number of distinct cell types that resolve into well-characterized cellular and functional identities. We also demonstrate that this powerful method can provide insights into the effect of inter- and trans- generational exposure to ethanol at tissue and cell-type specific resolution and identify the cells and molecular pathways that are most impacted by such exposures.

MATERIAL AND METHODS

Culture conditions and strains

The strain JK560 *fog-1(q253)* was used for sequencing and single molecule fluorescence *in situ* hybridization (smFISH) experiments. N2 (wild type) worms were used for embryonic lethality and acridine orange apoptosis experiments. The strain TY2441 (*Pxol-1:: gfp; rol-6(pRF4)*) was used for X chromosome aneuploidy experiments. Worms were cultured on standard nematode growth medium (NGM) plates streaked with single colony OP50 *E. coli* and maintained at 20°C. The generation of worms to be collected for single-nucleus analysis was moved to 25°C at the L1 stage and grown at 25°C for 48 hours until the beginning of day 2 of adulthood. To collect L1

larvae from the F1 generation, worms were synchronized by bleaching P0 gravid adults and having their F1 embryos subsequently grown for 16 hours at 20°C at which time all F1 were at the L1 stage. To collect L1 larvae from the F3 generation, the L1 larvae were collected through filtration using a 10µm nylon mesh filter (EDM Millipore NY1102500 and EDM Millipore SX00025000) which only allows L1 stage worms to pass through. L1 worms for both generations were kept for 48 hours at 25°C and then washed with five rounds of M9 buffer and centrifuged at 1,300g for 1 minute to pellet worms between each wash. After the final wash, worms were spun in a rotator with 1mL of M9 for 30 minutes to remove OP50 from the worms' gut. The worms were then allowed to settle by gravity for 5 minutes and the final compact worm pellet volume was adjusted to 30µL. The aforementioned strains were obtained from the *C. elegans* Genetics Center (CGC): JK560 *fog-1(q253)* I; TY2441 *yls34 (Pxol-1::gfp+rol-6 (pRF4))* (obtained by crossing *him-8(e1489)* out of TY2431); N2: wild-type.

***C. elegans* ethanol exposure**

For ethanol exposures, a population of gravid adult worms was bleached. The embryos obtained were plated on standard OP50 seeded NGM plates and allowed to grow to the L4 stage (approximately 50 hours post bleaching). Nematodes were exposed for 48 hours in a liquid culture containing M9 buffer solution, standard OP50 bacteria (10mg/mL), and ethanol at a final concentration of 0.05% or 0.50% in 15mL conical tubes. Following liquid exposure, the F1 progeny of the exposed P0 generation was split into two sets of plates, one for collecting the F1 adults and one for maintenance until the F3 generation. This scheme ensured the comparability of F1 and

F3 snRNA-seq data.

Single-nucleus dissociation

All single-nucleus dissociation steps were done at 4°C. A compact 30µL pellet of adult *JK560 C. elegans* (approximately 4,000 worms) was transferred to a prechilled Dounce homogenizer (Sigma Z378623-1EA) and homogenized for 10 strokes with 400µL of ice cold FA lysis buffer (50mM HEPES/NaOH pH 7.5, 1mM EDTA, 0.1% Triton X-100, 150mM NaCl, protease inhibitor 0.5X (Roche 11697498001), RNase inhibitor 0.2U/µL (Thermo Fisher 10777019), and RNase free water). Worms were homogenized for 10 strokes in a 1.5mL Wheaton Dounce homogenizer and for an additional 20 strokes (350µL FA buffer) with an Eppendorf Dounce homogenizer (Fisher 06-434) in a corkscrew fashion. Between each set of 10 homogenization strokes, debris was pelleted using 100g for 1 minute and supernatant containing nuclei was collected and pooled in a fresh 1.5mL low retention microcentrifuge tube.

After homogenization, the pooled supernatant containing nuclei was centrifuged at 100g for 1 minute to pellet remaining debris. The top 900µL of supernatant with nuclei was transferred to a fresh 1.5mL low retention microcentrifuge tube and washed once with 1% PBS BSA ((Thermo Fisher AM9624) that was filtered with a 0.22µm pressure filter (Thermo Scientific 03-377-26, Fisher SLGP033RS)). Nuclei were pelleted at 500g for 4 minutes, resuspended in 750-850µL 1% PBS-BSA, and then filtered using a 40µm Flowmi tip filter (Sigma-Aldrich BAH136800040-50EA).

Nuclei integrity was verified by staining single-nuclei isolations with DAPI and observing the nuclei under a fluorescent microscope. The nuclei did not have a frayed

appearance and were compact. Nuclei extractions were performed at 4°C in a timely fashion to prevent cellular transcription during the dissociation process. On average, a total of 1,200 nuclei is obtained per batch of 4,000 worms. Flow cytometry was used to ensure optimal nuclei concentration (700-1200 events/µl).

Single molecule fluorescence *in situ* hybridization

Single molecule fluorescence *in situ* hybridization (smFISH) was performed on F1 and F3 adults that were maintained, exposed, and filtered in a similar manner to animals used in the single-nucleus dissociation protocol. SmFISH was performed using the protocol developed by the Kimble Lab [29]. Probes were designed and ordered through Stellaris and are compiled in Table S1. Both probes were used at a final concentration of 0.25µM with approximately 100 dissected worms per condition. Samples were mounted on slides using fluoroshield with DAPI (Sigma-Aldrich F6057). Slides were imaged on the Leica SP8 confocal microscope. Fluorescence images were quantified using FISH-Quant v3 [30].

Embryonic lethality assessment, *xol-1::*gfp analysis, and apoptosis assay

Embryonic lethality was performed on wild-type N2 F1 and F3 worms. At both generations, L4s were singled out and moved onto individual 33mm plates. Embryonic lethality was performed by monitoring the number of embryos produced each day and the subsequent larvae that hatched from these embryos for each individual worm spanning its entire reproductive lifespan. *Pxol-1::gfp* analysis was done by fluorescent microscopy on 24-hours post-L4 F1 and F3 adults and the occurrence of GFP+

198 embryos (expressing *Pxol-1::gfp*) was recorded. The proportion of XOL-1::GFP+ was
199 calculated by dividing the number of worms with at least 1 GFP+ embryo by the total
200 number of worms analyzed [31]. Apoptosis assays were performed on wild-type N2
201 worms by Acridine Orange staining of synchronized adult hermaphrodites collected at
202 20-24 hours post-L4 at the F1 and F3 generations as previously described [32,33].
203
204 **Expanded Material and Methods, including computational analyses, can be found**
205 **in the supplemental information section.**
206
207 **RESULTS**
208 **SnRNA-seq identifies a wide array of defined cell types in the adult *C. elegans***
209 Intact nuclei were isolated from adult *fog-1(q253) C. elegans* raised at the
210 restrictive temperature of 25°C [34]. Since the focus of our study was on the
211 characterization of adult tissues response to ethanol, this sperm-defective strain was
212 used to prevent self-fertilization and the crowding of our snRNA-seq data with
213 embryonic cell types (see material and methods section). Briefly, worms were
214 synchronized and allowed to grow to day one of adulthood before mechanical nuclear
215 extraction (Figure 1A). Nuclei concentration was determined using flow cytometry and
216 nuclear integrity was assessed by high-resolution microscopy. Single nucleus RNA-seq
217 library preparation was performed using the 10X Genomics Chromium system followed
218 by 50 PE sequencing on the Illumina Novaseq 6000 platform. In total, we generated
219 transcriptomic data for 81,267 nuclei, each with more than 500 transcripts derived from
220 31 groups collected in 5 distinct batches. On average, 2,181 unique molecular

identifiers (UMIs) and 992 genes were detected per nucleus with high sequencing depth (90.3% average sequencing depth) (Figure S1).

The snRNA-seq reads were demultiplexed and aligned to the ENSEMBL ce10 *C. elegans* transcriptome to generate gene expression matrices using CellRanger (10x Genomics) (see supplemental material and methods). To mitigate the inclusion of debris-contaminated droplets and to correct for ambient RNA contamination, we also applied DIEM [35] and SoupX [36], respectively. DIEM identifies and removes droplets containing high levels of extranuclear RNA through modeling semi-supervised expectation maximization and outperforms other methods in snRNA-seq [35]. We then combined DIEM with SoupX which models contamination levels of snRNA-seq with ambient RNA and corrects expression for the remaining droplets. Using these stringent pipelines, we retained transcriptomic data from 41,750 droplets representing a median of 1,627 UMIs and 1,007 genes. A total of 31 discrete clusters were identified following batch/group effect correction by canonical correlation analysis (CCA) in Seurat v3 followed by Louvain clustering algorithm [37,38]. Log-normalized expression levels in t-distributed stochastic neighbor embedding (t-SNE) plot projections were used to visualize cell clusters in two dimensions and dot heatmap were used to visualize marker expression across different cell types (Figure 1B and Figure 2).

To facilitate unbiased cluster identification, gene enrichment (FDR<0.05) in each cluster was used to mine the Tissue enrichment, Gene Ontology, and Phenotype enrichment modules of WormBase [39] (Figure 1A). The output from these modules was cross-referenced with *in situ* expression data of the top enriched transcripts using the Nematode Expression Pattern Database (NEXTDB https://nematode.nig.ac.jp/) [40].

Comprehensive information for all 31 clusters that include top enriched and depleted genes, the 3 WormBase modules outputs, and representative examples from NEXTDB are presented in a dashboard (Supplemental data file 1). Examples are shown in Figure 2 alongside expression values of several known markers of each cell type showing notably high concordance. For example, cluster 23 is the only cluster showing a high expression level of the germline-specific transcripts *tra-2* [41], the meiotic-specific endonuclease *spo-11,* and the synaptonemal complex components *syp-1* and *syp-3* (as well as *syp-2* and *syp-4* not depicted here) [42,43]. In the adult *C. elegans* germline, the expression of *tra-2* is restricted to the most distal section of the germline and overlaps with that of the Notch signaling target *sygl-1* [29,44]. To test whether cluster 23 could correspond to the distal germline, we confirmed *sygl-1* expression by small molecule FISH (smFISH) as previously described [29] and compared its expression with its tSNE distribution (Figure S2). As expected, *sygl-1* showed a high expression level in the region corresponding to cluster 23 with some expression in other germline clusters which matched its smFISH distribution and published data [44] indicating that cluster 23 likely corresponds to the distal germline.

Similarly, cluster 3 specifically expresses all known markers of the spermatheca such as *fkh-6, ule-3, ule-5,* and also *ZK813.7* [45,46]. Marker analyses also revealed that sub-regionalization within clusters is apparent. For example, the three GABAergic neuron markers *unc-25, unc46,* and *unc-47* [47] resolve in one section of cluster 11 (Figure 2) which also expresses markers of cholinergic neurons (*e.g. cha-1* and *cho-1*) [48]. Also of note, based on WormBase's TEA analysis, several tissue- and cell- types are represented by multiple clusters (*e.g.* the germline represented by 6 clusters, the

intestine and epithelial system, represented by 3 cluster each) (Supplemental data file 1) likely reflective of the cellular heterogeneity underlying the composition of those tissues. Very few clusters (2/31), *i.e.* clusters 0 and 9, showed a lack of concordance between TEA, GO, and *in situ* data precluding assignment of a clear identity. All snRNA-seq data can be mined at: https://singlecell.broadinstitute.org/single_cell/reviewer_access/d94dacb1-9ab3-49f4-a5a0-392d8a0399ca (also see data availability section).

SnRNA-seq reveals broad impacts of inter-generational exposure to ethanol

We first applied snRNA-seq to identify the organism-wide transcriptional outcome of a parental 48-hour (L4 to end of day 1 of adulthood) exposure to two concentrations of ethanol (0.05% and 0.5%) or water control on the F1 adult progeny. These doses were chosen to circumscribe the wide range of human blood alcohol concentrations associated with low (0.05%) or high alcohol (0.5%) use respectively [49]. We first compared cell type proportion in the F1 following parental ethanol exposure and observed that broadly similar cell type distributions were observed across all treatment conditions (Figure S3). However, we observed a significant number of Differentially Expressed Genes (DEGs) (FDR<0.05) between treatment conditions (Figure 3A). Across all F1 clusters from the 0.05% ethanol exposure condition, we identified a total of 1,223 DEGs, including 583 uniformly upregulated DEGs, 520 uniformly downregulated DEGs, and 120 DEGs that were differentially up or down regulated in cluster specific ways (*i.e.* upregulated in some clusters but downregulated in other clusters) (Table S2). Surprisingly, compared to 0.05%, exposure to the higher ethanol

concentration of 0.5% resulted in fewer DEGs identified at the F1 (Table S3) with a total of 948 DEGs, including 430 uniformly upregulated DEGs, 407 uniformly downregulated DEGs, and 111 up- and down-regulated DEGs (Figure 3A).

Gene Ontology of the union of all DEGs revealed the enrichment of some functional categories that align with alcohol metabolism such as the GO category "carboxylic acid metabolic process" driven by the presence in the DEG list of several aldehyde dehydrogenases (Table 1 and Table S4), which catalyze the final step of ethanol metabolism from acetaldehyde into acetate. However, a major target of ethanol across exposure conditions and clusters is the translation machinery as exemplified by the deregulation of many ribosomal components and representing 5 of the top 10 GO categories, including the top 3 (Table S4). The inhibition of translation and the downregulation of genes encoding ribosomal subunits are a well described and conserved impact of alcohol exposure *in vitro* and in a variety of species from bacteria to humans [50–55]. In addition, reproductive pathways were amongst the top shared across exposure conditions at the F1, such as "gamete generation", "germ cell development", and "embryo development ending in birth or egg hatching" pathways (Table S4).

SnRNA-seq reveals tissue-specific DEGs from intergenerational (P0 to F1) exposure to ethanol

Next, we conducted cluster-specific DEG analysis to investigate cell type specific effects at the F1. Cluster-resolved DEG analysis indicated clearly distinct transcriptional

312 responses to parental ethanol exposure between cell types. While some genes were
313 consistently up-regulated (*atp-6, nduo-6*) or down-regulated (*vit-5*) across all clusters
314 between ethanol and water treatment, most DEGs showed cell type-specific restriction
315 as highlighted by the low overlap of the top DEGs per cluster (Figure S4, Table S2 and
316 S3). To rank order the F1 clusters by sensitivity to ethanol exposure, we employed a
317 Euclidean distance analysis [56,57], which estimates the degree of transcriptomic shifts
318 between exposure and control groups (see Supplemental Material and Methods).
319 Several clusters (1, 15, and 30) with an assigned germline identity based on
320 TEA/GO/Phenotype enrichment analyses and NEXTDB (Supplemental File 1) showed
321 some of the largest degree of transcriptomic shifts at the F1 generation under 0.5%
322 ethanol exposure condition (Figure 3B). Other cluster categories that appeared most
323 affected included clusters related to muscle function such as cluster 2 and cluster 17,
324 both carrying striated muscle cell identity. The degree of transcriptomic shift was much
325 less pronounced following 0.05% ethanol exposure compared to 0.5% ethanol,
326 suggesting a dose-dependent transcriptomic response across cell types.

327 We hypothesized that while most DEGs are cell type-specific, genes implicated
328 in ethanol metabolism may show a more uniform response across clusters. Thus, we
329 investigated the expression of genes involved in ethanol metabolism, including 3 distinct
330 alcohol dehydrogenase (*sodh-1*, H24K24.3, ZK829.7) and 10 aldehyde dehydrogenase
331 (*alh-3, -4, -7* through *-13*), whose expression was detectable in our datasets (Figure
332 S5). Contrary to our expectations, of the 13 genes examined, only 5 showed significant
333 changes in expression (FDR < 0.05) and did so in a cluster- and dose- dependent
334 fashion. For example, *sodh-1* was upregulated in cluster 13 and cluster 18 under the

335 0.05% exposure condition but was downregulated in cluster 2 and cluster 27 at 0.5%.
336 Notably, the cell types showing the highest increase in ethanol metabolism genes were
337 not the cell types that were the least sensitive to ethanol and vice versa, suggesting that
338 the upregulation of ethanol metabolism genes in the F1 does not protect a tissue from
339 the inter-generational impact of exposure (compare Figure 3B and S5).

340 At the F1, the majority of the clusters reaching statistical significance (FDR<0.05)
341 after 0.5% ethanol exposure in our Euclidean Distance analysis displayed a germline
342 identity, *e.g.* clusters 1, 12, 15, 23, 30. Thus, we next examined whether reproduction-
343 related phenotypes were significantly over-represented in our dataset. We analyzed the
344 top 10 most shared WormBase phenotypes across cell types with significantly altered
345 Euclidean distance and identified several phenotypic terms related to reproduction (*e.g.*
346 “diplotene region organization variant”, “pachytene region organization variant”, “germ
347 cell compartment expansion variant”) that are mildly upregulated in germline cluster 1
348 but strongly and uniformly downregulated in germline cluster 12 (Figure 4A). Finally, we
349 examined whether the DEGs across the sensitive cell types were enriched in specific
350 phenotypes by comparing the DEGs’ phenotype enrichment outcome with all
351 WormBase phenotypes. This analysis revealed that our dataset has a significantly
352 higher proportion of phenotypes related to reproductive system development, cellular
353 development, and morphology categories among both treatment groups (Figure 4B).

354 Since the germline appears to be a major target for ethanol at the F1 and F3
355 generations, we validated the magnitude and directionality of the transcriptional impact
356 of ethanol exposure in that tissue. For example, in our snRNA-seq dataset, *tra-2*
357 showed a significant downregulation of its expression in cluster 23 in the F1 under 0.5%

ethanol exposure (Figure 3D, Table S3, 0.60-fold change, adjusted P value = 0.003). We performed smFISH in dissected F1 germlines followed by quantification using FISH-quant (Figure 3F-I). We observed a congruent 0.47-fold downregulation of *tra-2* level ($P<0.05$). Conversely, at the F3 under 0.5% ethanol exposure condition, *mex-3* was significantly upregulated in our snRNA-seq dataset in germline cluster 12 (Figure 3E, Table S6, 1.58-fold change, adjusted P value = 0.008). Cluster 12 also as a meiotic germline identity based on GO enrichment (Supplemental file 1). SmFISH indicated an upregulation of *mex-3* in the mid-pachytene region of F3 *C. elegans* gonads (2.19-fold, $P<0.001$).

Together, these results indicate a strong intergenerational impact of alcohol in *C. elegans* on a variety of cell types including those that belong to the germline.

Transgenerational (P0 to F3) impact of ethanol

We extended our snRNA-seq approach to the F3 generation to capture the transgenerational effect of P0 exposure to ethanol. Similarly to the F1, no overt impact on cell type distributions was observed (Figure S3). Across all clusters at the F3 stemming from a P0 0.05% ethanol exposure, a total of 798 unique Differentially Expressed Genes (DEGs), 366 unique upregulated DEGs, 369 unique downregulated DEGs satisfying an FDR<0.05 and 63 DEGs that were differentially up or down regulated in cluster specific ways (Figure 3A, Table S5). For 0.5% ethanol, a total of 918 unique Differentially Expressed Genes (DEGs) were identified comprising 402 unique upregulated DEGs, 422 unique downregulated DEGs satisfying an FDR<0.05 and 94 DEGs that were differentially up or down regulated in cluster specific ways (Figure 3A,

Table S6).

Gene Ontology analysis of all F3 DEGs revealed the enrichment of some functional categories that align with alcohol metabolism. These were exemplified by GO categories such as “carboxylic acid metabolic process”, “drug metabolic process”, and “small molecule catabolic process” driven in part by the presence in our DEG list of alcohol dehydrogenase genes, *sodh-1* and *hphd-1*, which catalyze the first step of ethanol metabolism from ethanol to acetaldehyde, as well as aldehyde dehydrogenase genes, *alh-8* and *alh-13*, which catalyzes the second step of ethanol metabolism from acetaldehyde into acetate, in both exposure groups as compared to water at the F3 (Table 1 and Table S4). Other highly enriched GO terms were “structural molecule activity”, “cytoskeleton organization”, “translation” and reproductive GO categories “embryo development ending in birth or egg hatching” and “sexual reproduction”.

Cell type-specific transgenerational response to ethanol

Next, we conducted cluster specific DEG analysis to investigate ethanol’s transgenerational effects. While the majority of top DEGs at the F1 were up-regulated, in comparison, the majority of the top DEGs found at the F3 were down-regulated, especially at the 0.5% ethanol exposure condition (Figure S6). These top DEGs showed remarkable cell type specificity as highlighted by their low overlap across clusters. We assessed the sensitivity of individual clusters by measuring their Euclidean distance (Figure 3C). Notably, compared to the F1 results, more clusters reached the cut-off of FDR<0.05 from 0.5% exposure at the F3. While changes in the relative order of the clusters were observed between F3 and F1, several germline clusters showed some of

the largest transcriptomic shifts including cluster 1 which remained the cluster the most transcriptionally affected by ethanol (Figure 3C).

The examination of F3 DEGs through the WormBase phenotype enrichment tool revealed a strong alteration of different phenotypes under the 0.5% ethanol exposure condition, albeit in a less uniform fashion across clusters (Figure 4C,D). The phenotype pachytene region organization variant was downregulated in cluster 1 but not in other germline clusters, suggesting a lasting but weakened impact of ethanol exposure effect at the F3. A comparison of phenotype proportion between our dataset and all phenotypes, revealed a persistent enrichment in the F3 of the phenotypic categories described in the F1 including a higher proportion of reproductive system development variant at 0.5% ethanol. By contrast to the F1, no phenotypic category reached significance under the 0.05% ethanol exposure condition, confirming the weakened impact of ethanol at the F3.

Functional outcomes of ethanol's inter- and trans- generational transcriptional impacts.

The presence of several germline clusters amongst the most transcriptionally impacted clusters as well as the enrichment of some reproductive phenotypes at the F1 and F3 suggested that ethanol exposure may have a significant functional impact on reproduction at these generations. To test this hypothesis, we measured three hallmarks of reproductive health in *C. elegans*: germline apoptosis by acridine orange staining [32], the proper segregation of chromosomes during meiosis by monitoring the segregation of the X chromosome [58], and the viability of produced embryos through

plate phenotyping [33,59]. All three reproductive measures were significantly upregulated at either 0.05% or 0.5% ethanol exposures in the F1 and in the F3 compared to the water control, remarkably, with no consistent dose-response relationship (Figure 5). Analysis of germline apoptosis through acridine orange staining revealed a 2-fold increase in the number of apoptotic nuclei per gonad in F1 worms who were exposed to 0.05% ethanol at the P0 ($N=5$, $P<0.05$) and a 2.7-fold increase in those who were exposed to 0.50% ethanol ($N=5$, $P<0.0001$) when compared to water. Similarly, at the F3, a 1.9-fold increase for both ethanol exposure conditions was observed when compared to water ($N=4$-5, $P<0.001$). Next, we monitored chromosome segregation through the segregation of the X chromosome using a strain carrying the *Pxol-1::gfp* reporter [31,58]. Chromosomes that fail to properly segregate during meiosis result in embryos with aneuploidies [43]. Here, we monitored aneuploidy *via* the incidence of male (XO) embryos which are caused by mis-segregation of the X-chromosome and marked by the expression of the male-specific *xol-1* promoter driving GFP. Analysis at the F1 identified a significant increase in the incidence of GFP-positive embryos for both ethanol exposure conditions when compared to water with a 2.6-fold increase in the proportion of worms with at least one GFP-positive embryo at 0.05% ethanol exposure ($N=6$-7, $P<0.01$) and a 2.8-fold increase at 0.50% ethanol exposure ($N=6$-7, $P<0.01$). The incidence of GFP-positive embryos further increased at the F3 with a 4-fold increase at 0.05% ethanol exposure ($N=6$-7, $P<0.01$) and a 4.3-fold increase at 0.50% ethanol exposure ($N=6$-7, $P<0.001$). Together, these results indicate a profound impact of inter- and trans-generational alcohol exposure on the nematode's reproductive function congruent with the outcome of our snRNA-seq analysis.

DISCUSSION

We performed single-nucleus RNA-seq approach in the adult *C. elegans* nematode and identified a large number of transcriptionally distinct cell types. By applying this approach to the study of the inter- and trans-generational impacts of ethanol exposure, we also demonstrate its utility in achieving a nuanced understanding of transcriptional responses to environmental cues.

We circumvented some of the drawbacks associated with single nucleus approaches by employing multiple data clean-up pipelines to identify and remove debris-contaminated droplets and spurious signal from ambient RNA, a common artifact of snRNA-seq [35,36]. This stringent approach removed approximately half of all droplets but still generated a robust number of UMI and genes per nucleus when compared with other studies [60]. Our approach also generated a larger number of clusters corresponding to cell types previously under-represented in single cell RNA-seq studies in *C. elegans* because of their lack of cellularization, *e.g.* meiotic stages of the germline and hypodermal cells.

Our approach nonetheless has several limitations. By working in a *fog-1* mutant background, we were not able to identify sperm cells, highlighted by the absence of expression of canonical sperm markers in our dataset. This was considered a necessary trade-off to avoid the production of embryos and the crowding of snRNA-seq data with a large and diverse number of embryonic cell types. While it is possible that *fog-1's* absence alters the transcriptional landscape of the germline, *fog-1(q253)* was chosen specifically because of the normal morphology and staging of the hermaphrodite

germline in the *fog-1* mutant background [34]. Secondly, for a small number of clusters, tissue enrichment analysis did not delineate a clear cell type identity (2/31 clusters) either representing cell types with mixed identities or cell types for which other clustering methods would be beneficial. Nonetheless, the large majority of clusters bore a distinctive tissue identity not only corroborated by GO and phenotype enrichment analyses but also by the tissue-specific *in situ* expression pattern of genes showing the highest degree of cluster specificity.

The application of our snRNA-seq approach to the study of ethanol's response across generations highlighted the complexity of organisms' response to environmental cues. This aspect was exemplified by the diversity and specificity of GO categories by clusters (Table S4) and by the low degree of overlap of top DEGs between clusters (Figure S4 and S6). Because of their high ranking in the Euclidean analysis in both F1 and F3 generations, several tissue types stood out as being particularly affected by ethanol: the muscle system, neurons, and the germline. The direct impact of alcohol on skeletal and cardiac muscle cells is well described and a common outcome of chronic alcohol use [61–63]. An intergenerational effect of prenatal alcohol exposure on the musculature and muscle function has also been demonstrated and is referred to as fetal alcohol myopathy [64,65]. Interestingly, a proposed mechanism for this induced muscle cell dysfunction is an alteration of protein synthesis [66,67] which is represented by several GO categories (*e.g.* "peptide metabolic process", "peptide biosynthetic process", "translation") in our DEG pathway analysis (Table S4). Supplementation of amino acids to facilitate translation processes might be tested as a method of improving the impact of ethanol on the F1 muscle cells. The mechanisms of transgenerational impact of

alcohol on F3 musculature, however, is unclear and has not been previously described.

Similarly, cluster 11 which comprises GABAergic (*e.g. unc-25*$^{+}$) and some cholinergic neurons (*e.g. cha-1*$^{+}$*)* is also identified as being significantly altered by 0.5% ethanol at the F1 and F2. Interestingly, GABAergic neurons are also a well-known target of direct and intergenerational alcohol exposure in which alcohol leads to over stimulation of the GABA system leading to dampening of neuronal excitability [68–71]. To a lesser extent, cholinergic signaling has also been implicated in the intergenerational impact of ethanol on the nervous system [72–74]. Since in *C. elegans*, direct alcohol exposure is associated with a deregulation of cholinergic signaling and locomotory behavior [16,75], it will be important to also investigate the role of GABA signaling and its interaction with cholinergic signaling in regulating locomotion not only in a direct exposure paradigm but also across generations.

Germline clusters were ranked the highest in the Euclidean distance analysis at the F1 and F3 generations. We therefore focused our validation experiments on the germline and reproduction. Direct ethanol exposure has been known to cause aneuploidy in mammalian germ cells for many years [76–78], however whether these effects extend to the F1's germline has remained uncertain. Our results clearly indicate that in *C. elegans*, both low and high concentrations of ethanol have a profound impact on reproductive function (germ cell apoptosis, aneuploidy, embryonic lethality) and that these impacts extend transgenerationally. We have recently demonstrated that the transgenerational reproductive effects of the environmental chemical Bisphenol A requires the alteration of the repressive histone marks H3K9me3 and H3K27me3 [23,25]. Intergenerational alcohol exposure, on the other hand, has been shown to lead

519 to histone hyperacetylation through the metabolism of ethanol into acetate [79]. Thus, it
520 is plausible that alcohol's inter- and trans-generational outcomes described here may be
521 initiated by the over-acetylation of histone in the germline. Finally, while we validated
522 ethanol's impacts on several DEGs by smFISH in the germline, a more comprehensive
523 DEG validation in other tissues will be needed as well as comparison with cell type-
524 specific intergenerational and transgenerational ethanol transcriptional outcome in
525 mammalian models when such data becomes available.

526 Together, the application of snRNA-seq to the adult *C. elegans* represents a
527 powerful approach for the comprehensive identification of cell types in the nematode
528 and for probing the transcriptional impact of physiological and environmental changes.

529

530 **DATA AVAILABILITY**

531 All raw data is accessible on NCBI's Gene Expression Omnibus (GEO), at:
532 https://www.ncbi.nlm.nih.gov/geo/query/acc.cgi?acc=GSE208229

533

534 The data is also available through the Broad Single Cell Portal:
535 https://singlecell.broadinstitute.org/single_cell/study/SCP922/single-nucleus-resolution-
536 mapping-of-the-adult-c-elegans-and-its-application-to-elucidate-inter-and-trans-
537 generational-response-to-alcohol

538

539 **ACKNOWLEDGEMENTS**

540 The authors would like to thank Doug Arneson for input on single-nucleus sequencing
541 parameters; Ingrid Cely, In Sook Ahn, and Graciel Diamante for discussions and

trouble-shooting advice; Eyal Ben David for advice on single-cell/nuclei dissociation methods; Jessica Scholes, Jeffrey Calim, Felicia Codrea, and Salem Haile for guidance with single-nucleus cytometry; Michael Mashock and Marco De Simone for their library preparation and sequencing expertise. Matteo Pellegrini for advice and input on data analysis. We thank Judith Kimble, Tina Lynch, and Sarah Crittenden for advice on smFISH and providing the *sygl-1* probe. The *Caenorhabditis* Genetics Center (CGC) provided the strains used in this study. We thank Yuji Kohara for permission to use NEXTDB *in situ* data.

FUNDING

LT is supported by the NIH Training Grant in Genomic Analysis and Interpretation T32 HG002536; YWC is supported by the UCLA Eureka fellowship and Burroughs Wellcome Fund Inter-school Training Program in Chronic Diseases; PA is supported by NIEHS R01 ES027487, NIAAA R21 AA024889, the John Templeton Foundation, and the Burroughs Wellcome Innovation in Regulatory Science Award. EDVB and PWS are supported by U24HG002223.

REFERENCES

1. Denny L, Coles S, Blitz R. Fetal alcohol syndrome and fetal alcohol spectrum disorders. Am Fam Physician [Internet]. 2017 Oct 15 [cited 2022 Jul 7];96(8):515–22 PMID29094891. Available from: https://www.aafp.org/pubs/afp/issues/2017/1015/p515.html

2. Caputo C, Wood E, Jabbour L. Impact of fetal alcohol exposure on body systems: A systematic review [Internet]. Vol. 108, Birth Defects Research Part C - Embryo Today: Reviews. 2016.108(2):174–80 PMID27297122. Available from: http://dx.doi.org/10.1002/bdrc.21129

3. La Vignera S, Condorelli RA, Balercia G, Vicari E, Calogero AE. Does alcohol have any effect on male reproductive function? A review of literature [Internet]. Vol. 15, Asian Journal of Andrology. 2013.15(2):221–5 PMID23274392. Available from: http://dx.doi.org/10.1038/aja.2012.118

4. Strategic plan 2017-2021 [Internet]. [cited 2022 Jul 7]. Available from: https://www.niaaa.nih.gov/strategic-plan

5. Abbott CW, Rohac DJ, Bottom RT, Patadia S, Huffman KJ. Prenatal Ethanol Exposure and Neocortical Development: A Transgenerational Model of FASD. Cereb Cortex [Internet]. 2018;28(8):2908–21 PMID29106518. Available from: https://www.ncbi.nlm.nih.gov/pubmed/29106518

6. Bozler J, Kacsoh BZ, Bosco G. Transgeneratonal inheritance of ethanol preference is caused by maternal NPF repression. Elife [Internet]. 2019 Jul 9;8:e45391 PMID31287057PMC6615861. Available from: https://elifesciences.org/articles/45391

7. Gangisetty O, Palagani A, Sarkar DK. Transgenerational inheritance of fetal alcohol exposure adverse effects on immune gene interferon-□. Clin Epigenetics [Internet]. 2020 May 24;12(1):70 PMID32448218PMC7245772. Available from: http://dx.doi.org/10.1186/s13148-020-00859-9

8. Bottom RT, Kozanian OO, Rohac DJ, Erickson MA, Huffman KJ. Transgenerational effects of prenatal ethanol exposure in prepubescent mice. Front Cell Dev Biol [Internet]. 2022 Mar 21;10:812429 PMID35386207PMC8978834. Available from: http://dx.doi.org/10.3389/fcell.2022.812429

9. Nizhnikov ME, Popoola DO, Cameron NM. Transgenerational Transmission of the Effect of Gestational Ethanol Exposure on Ethanol Use-Related Behavior. Alcohol Clin Exp Res [Internet]. 2016;40(3):497–506 PMID26876534. Available from: http://dx.doi.org/10.1111/acer.12978

10. Hollander J, McNivens M, Pautassi RM, Nizhnikov ME. Offspring of male rats exposed to binge alcohol exhibit heightened ethanol intake at infancy and alterations in T-maze performance. Alcohol [Internet]. 2019;76:65–71 PMID30583252. Available from: http://dx.doi.org/10.1016/j.alcohol.2018.07.013

11. Lam MKP, Homewood J, Taylor AJ, Mazurski EJ. Second generation effects of maternal alcohol consumption during pregnancy in rats. Prog Neuropsychopharmacol Biol Psychiatry [Internet]. 2000;24(4):619–31 PMID10958155. Available from: http://dx.doi.org/10.1016/S0278-5846(00)00097-X

12. Yohn NL, Bartolomei MS, Blendy JA. Multigenerational and transgenerational inheritance of drug exposure: The effects of alcohol, opiates, cocaine, marijuana, andnicotine [Internet]. Vol. 118, Progress in Biophysics and Molecular Biology. 2015.118(1–2):21–33 PMID25839742. Available from: http://dx.doi.org/10.1016/j.pbiomolbio.2015.03.002

13. Patten AR, Fontaine CJ, Christie BR. A comparison of the different animal models of fetal alcohol spectrum disorders and their use in studying complex behaviors [Internet]. Vol. 2, Frontiers in Pediatrics. 2014.2(SEP). Available from: http://dx.doi.org/10.3389/fped.2014.00093

14. Mitchell PH, Bull K, Glautier S, Hopper NA, Holden-Dye L, O'Connor V. The concentration-dependent effects of ethanol on Caenorhabditis elegans behaviour. Pharmacogenomics J [Internet]. 2007 Dec;7(6):411–7 PMID17325734. Available from: http://dx.doi.org/10.1038/sj.tpj.6500440

15. Lee J, Jee C, McIntire SL. Ethanol preference in C. elegans. Genes Brain Behav [Internet]. 2009;8(6):578–85 PMID19614755. Available from: http://dx.doi.org/10.1111/j.1601-183X.2009.00513.x

16. McIntire SL. Ethanol [Internet]. WormBook : the online review of C. elegans biology. 2010.:1–6 PMID20432508. Available from: http://dx.doi.org/10.1895/wormbook.1.40.1

17. Topper SM, Aguilar SC, Topper VY, Elbel E, Pierce-Shimomura JT. Alcohol disinhibition of behaviors in C. elegans. PLoS One [Internet]. 2014;9(3) PMID24681782. Available from: http://dx.doi.org/10.1371/journal.pone.0092965

18. Pandey P, Singh A, Kaur H, Ghosh-Roy A, Babu K. Increased dopaminergic neurotransmission results in ethanol dependent sedative behaviors in Caenorhabditis elegans. PLoS Genet [Internet]. 2021;17(2):e1009346 PMID33524034. Available from: http://dx.doi.org/10.1371/journal.pgen.1009346

19. Alaimo JT, Davis SJ, Song SS, Burnette CR, Grotewiel M, Shelton KL, et al. Ethanol Metabolism and Osmolarity Modify Behavioral Responses to Ethanol in C. elegans. Alcohol Clin Exp Res [Internet]. 2012;36(11):1840–50 PMID22486589. Available from: http://dx.doi.org/10.1111/j.1530-0277.2012.01799.x

20. Cao J, Packer JS, Ramani V, Cusanovich DA, Huynh C, Daza R, et al. Comprehensive single-cell transcriptional profiling of a multicellular organism. Science [Internet]. 2017;357(6352):661–7 PMID28818938. Available from: http://dx.doi.org/10.1126/science.aam8940

21. Packer JS, Zhu Q, Huynh C, Sivaramakrishnan P, Preston E, Dueck H, et al. A lineage-resolved molecular atlas of C. Elegans embryogenesis at single-cell resolution. Science [Internet]. 2019;365(6459) PMID31488706. Available from: http://dx.doi.org/10.1126/science.aax1971

22. Taylor SR, Santpere G, Weinreb A, Barrett A, Reilly MB, Xu C, et al. Molecular topography of an entire nervous system. Cell [Internet]. 2021 Aug 5;184(16):4329-4347.e23 PMID34237253PMC8710130. Available from: http://dx.doi.org/10.1016/j.cell.2021.06.023

23. Camacho J, Allard P. Histone Modifications: Epigenetic Mediators of Environmental

645 Exposure Memory. Epigenetics Insights. 2018;11.

646 24. Weinhouse C, Truong L, Meyer JN, Allard P. Caenorhabditis elegans as an
647 emerging model system in environmental epigenetics. Environ Mol Mutagen
648 [Internet]. 2018;59(7):560–75 PMID30091255. Available from:
649 http://dx.doi.org/10.1002/em.22203

650 25. Camacho J, Truong L, Kurt Z, Chen Y-W, Morselli M, Gutierrez G, et al. The
651 Memory of Environmental Chemical Exposure in C. elegans Is Dependent on the
652 Jumonji Demethylases jmjd-2 and jmjd-3/utx-1. Cell Rep [Internet]. 2018 May
653 22;23(8):2392–404 PMID29791850PMC6003705. Available from:
654 http://dx.doi.org/10.1016/j.celrep.2018.04.078

655 26. Kelly WG. Transgenerational epigenetics in the germline cycle of Caenorhabditis
656 elegans. Epigenetics Chromatin [Internet]. 2014;7(1):6 PMID24678826. Available
657 from: http://dx.doi.org/10.1186/1756-8935-7-6

658 27. Kishimoto S, Uno M, Okabe E, Nono M, Nishida E. Environmental stresses induce
659 transgenerationally inheritable survival advantages via germline-to-soma
660 communication in Caenorhabditis elegans. Nat Commun [Internet]. 2017;8:14031
661 PMID28067237. Available from: https://www.ncbi.nlm.nih.gov/pubmed/28067237

662 28. Klosin A, Casas E, Hidalgo-Carcedo C, Vavouri T, Lehner B. Transgenerational
663 transmission of environmental information in C. elegans. Science [Internet].
664 2017;356(6335):320–3 PMID28428426. Available from:
665 https://www.ncbi.nlm.nih.gov/pubmed/28428426

666 29. Lee C, Seidel HS, Lynch TR, Sorensen EB, Crittenden SL, Kimble J. Single-
667 molecule RNA Fluorescence in situ Hybridization (smFISH) in Caenorhabditis
668 elegans. Bio Protoc [Internet]. 2017 Jun 20;7(12):e2357
669 PMID34541104PMC8410355. Available from:
670 http://dx.doi.org/10.21769/BioProtoc.2357

671 30. Mueller F, Senecal A, Tantale K, Marie-Nelly H, Ly N, Collin O, et al. FISH-quant:
672 automatic counting of transcripts in 3D FISH images. Nat Methods [Internet]. 2013
673 Apr 28 [cited 2022 Jul 10];10(4):277–8 PMID23538861. Available from:
674 https://www.nature.com/articles/nmeth.2406

675 31. Allard P, Kleinstreuer NC, Knudsen TB, Colaiacovo MP. A Screening Platform for
676 the Rapid Assessment of Chemical Disruption of Germline Function. Environ Health
677 Perspect [Internet]. 2013;2013/04/23 PMID23603051. Available from:
678 http://dx.doi.org/10.1289/ehp.1206301

679 32. Gartner A, Boag PR, Blackwell TK. Germline survival and apoptosis [Internet].
680 WormBook : the online review of C. elegans biology. 2008.:1–20 PMID18781708.
681 Available from: http://dx.doi.org/10.1895/wormbook.1.145.1

682 33. Chen Y, Shu L, Qiu Z, Lee DY, Settle SJ, Que Hee S, et al. Exposure to the BPA-

683 Substitute Bisphenol S Causes Unique Alterations of Germline Function. PLoS
684 Genet [Internet]. 2016;12(7) PMID27472198. Available from:
685 http://dx.doi.org/10.1371/journal.pgen.1006223

686 34. Barton MK, Kimble J. fog-1, a regulatory gene required for specification of
687 spermatogenesis in the germ line of Caenorhabditis elegans. Genetics. 1990;

688 35. Alvarez M, Rahmani E, Jew B, Garske KM, Miao Z, Benhammou JN, et al.
689 Enhancing droplet-based single-nucleus RNA-seq resolution using the semi-
690 supervised machine learning classifier DIEM. Sci Rep [Internet]. 2020;
691 PMID32620816. Available from: http://dx.doi.org/10.1038/s41598-020-67513-5

692 36. Young MD, Behjati S. SoupX removes ambient RNA contamination from droplet-
693 based single-cell RNA sequencing data. Gigascience [Internet]. 2020;
694 PMID33367645. Available from: http://dx.doi.org/10.1093/gigascience/giaa151

695 37. Stuart T, Butler A, Hoffman P, Hafemeister C, Papalexi E, Mauck WM, et al.
696 Comprehensive Integration of Single-Cell Data. Cell [Internet]. 2019;
697 PMID31178118. Available from: http://dx.doi.org/10.1016/j.cell.2019.05.031

698 38. Waltman L, Van Eck NJ. A smart local moving algorithm for large-scale modularity-
699 based community detection. European Physical Journal B [Internet]. 2013;
700 Available from: http://dx.doi.org/10.1140/epjb/e2013-40829-0

701 39. Angeles-Albores D, N Lee RY, Chan J, Sternberg PW. Tissue enrichment analysis
702 for C. elegans genomics. BMC Bioinformatics [Internet]. 2016 Sep 13;17(1):366
703 PMID27618863PMC5020436. Available from: http://dx.doi.org/10.1186/s12859-
704 016-1229-9

705 40. [cited 2021 Nov 8]. Available from: http://nematode.lab.nig.ac.jp/

706 41. Hu S, Skelly LE, Kaymak E, Freeberg L, Lo T-W, Kuersten S, et al. Multi-modal
707 regulation of C. elegans hermaphrodite spermatogenesis by the GLD-1-FOG-2
708 complex. Dev Biol [Internet]. 2019 Feb 15;446(2):193–205 PMID30599151.
709 Available from:
710 https://www.sciencedirect.com/science/article/pii/S0012160618301866

711 42. Dernburg AF, McDonald K, Moulder G, Barstead R, Dresser M, Villeneuve AM.
712 Meiotic recombination in C. elegans initiates by a conserved mechanism and is
713 dispensable for homologous chromosome synapsis. Cell [Internet]. 1998;94(3):387–
714 98 PMID9708740. Available from: http://dx.doi.org/10.1016/S0092-8674(00)81481-
715 6

716 43. Colaiacovo MP. The many facets of SC function during C. elegans meiosis.
717 Chromosoma [Internet]. 2006 Jun;115(3):195–211. Available from:
718 http://www.ncbi.nlm.nih.gov/entrez/query.fcgi?cmd=Retrieve&db=PubMed&dopt=Cit
719 ation&list_uids=16555015

44. Shin H, Haupt KA, Kershner AM, Kroll-Conner P, Wickens M, Kimble J. SYGL-1 and LST-1 link niche signaling to PUF RNA repression for stem cell maintenance in Caenorhabditis elegans. PLoS Genet [Internet]. 2017 Dec;13(12):e1007121 PMID29232700PMC5741267. Available from: http://dx.doi.org/10.1371/journal.pgen.1007121

45. Gissendanner CR, Kelley K, Nguyen TQ, Hoener MC, Sluder AE, Maina CV. The Caenorhabditis elegans NR4A nuclear receptor is required for spermatheca morphogenesis. Dev Biol [Internet]. 2008 Jan 15;313(2):767–86 PMID18096150PMC3845373. Available from: http://dx.doi.org/10.1016/j.ydbio.2007.11.014

46. Kalis AK, Kroetz MB, Larson KM, Zarkower D. Functional genomic identification of genes required for male gonadal differentiation in Caenorhabditis elegans. Genetics [Internet]. 2010 Jun 1 [cited 2022 Jul 9];185(2):523–35 PMID20308279PMC2881134. Available from: https://academic.oup.com/genetics/article/185/2/523/6096927

47. Jorgensen EM. GABA. WormBook [Internet]. 2005 Aug 31;1–13 PMID18050397PMC4781266. Available from: http://dx.doi.org/10.1895/wormbook.1.14.1

48. Rand JB. Acetylcholine. WormBook [Internet]. 2007 Jan 30;1–21 PMID18050502PMC4781110. Available from: http://dx.doi.org/10.1895/wormbook.1.131.1

49. Martinez-Hurtado J, Calo-Fernandez B, Vazquez-Padin J. Preventing and Mitigating Alcohol Toxicity: A Review on Protective Substances. Beverages [Internet]. 2018;4(2):39. Available from: http://dx.doi.org/10.3390/beverages4020039

50. David ET, Fischer I, Moldave K. Studies on the effect of ethanol on eukaryotic protein synthesis in vitro. J Biol Chem [Internet]. 1983 Jun 25;258(12):7702–6 PMID6553051. Available from: http://dx.doi.org/10.1016/s0021-9258(18)32236-1

51. Cahill A, Baio DL, Ivester P, Cunningham CC. Differential effects of chronic ethanol consumption on hepatic mitochondrial and cytoplasmic ribosomes. Alcohol Clin Exp Res [Internet]. 1996 Nov;20(8):1362–7 PMID8947311. Available from: http://dx.doi.org/10.1111/j.1530-0277.1996.tb01135.x

52. Vary TC, Lynch CJ, Lang CH. Effects of chronic alcohol consumption on regulation of myocardial protein synthesis. Am J Physiol Heart Circ Physiol [Internet]. 2001 Sep;281(3):H1242-51 PMID11514293. Available from: http://dx.doi.org/10.1152/ajpheart.2001.281.3.H1242

53. Karinch AM, Martin JH, Vary TC. Acute and chronic ethanol consumption differentially impact pathways limiting hepatic protein synthesis. Am J Physiol Endocrinol Metab [Internet]. 2008 Jul;295(1):E3-9 PMID18334613PMC2493597. Available from: http://dx.doi.org/10.1152/ajpendo.00026.2008

54. Haft RJF, Keating DH, Schwaegler T, Schwalbach MS, Vinokur J, Tremaine M, et al. Correcting direct effects of ethanol on translation and transcription machinery confers ethanol tolerance in bacteria. Proc Natl Acad Sci U S A [Internet]. 2014 Jun 24;111(25):E2576-85 PMID24927582PMC4078849. Available from: http://dx.doi.org/10.1073/pnas.1401853111

55. Berres ME, Garic A, Flentke GR, Smith SM. Transcriptome profiling identifies ribosome biogenesis as a target of alcohol teratogenicity and vulnerability during early embryogenesis. PLoS One [Internet]. 2017 Jan 3;12(1):e0169351 PMID28046103PMC5207668. Available from: http://dx.doi.org/10.1371/journal.pone.0169351

56. Arneson D, Zhang G, Ying Z, Zhuang Y, Byun HR, Ahn IS, et al. Single cell molecular alterations reveal target cells and pathways of concussive brain injury. Nat Commun [Internet]. 2018;9(1) PMID30254269. Available from: http://dx.doi.org/10.1038/s41467-018-06222-0

57. Liu W, Venugopal S, Majid S, Ahn IS, Diamante G, Hong J, et al. Single-cell RNA-seq analysis of the brainstem of mutant SOD1 mice reveals perturbed cell types and pathways of amyotrophic lateral sclerosis. Neurobiol Dis [Internet]. 2020;141 PMID32360664. Available from: http://dx.doi.org/10.1016/j.nbd.2020.104877

58. Nicoll M, Akerib CC, Meyer BJ. X-chromosome-counting mechanisms that determine nematode sex. Nature [Internet]. 1997;388(6638):200–4. Available from: http://www.ncbi.nlm.nih.gov/entrez/query.fcgi?cmd=Retrieve&db=PubMed&dopt=Citation&list_uids=9217163

59. MacQueen AJ, Colaiacovo MP, McDonald K, Villeneuve AM. Synapsis-dependent and -independent mechanisms stabilize homolog pairing during meiotic prophase in C. elegans. Genes Dev [Internet]. 2002;16(18):2428–42. Available from: http://www.ncbi.nlm.nih.gov/entrez/query.fcgi?cmd=Retrieve&db=PubMed&dopt=Citation&list_uids=12231631

60. Selewa A, Dohn R, Eckart H, Lozano S, Xie B, Gauchat E, et al. Systematic Comparison of High-throughput Single-Cell and Single-Nucleus Transcriptomes during Cardiomyocyte Differentiation. Scientific Reports [Internet]. 2020; Available from: http://dx.doi.org/10.1038/s41598-020-58327-6

61. Urbano-Marquez A, Estruch R, Navarro-Lopez F, Grau JM, Mont L, Rubin E. The effects of alcoholism on skeletal and cardiac muscle. N Engl J Med [Internet]. 1989 Feb 16;320(7):409–15 PMID2913506. Available from: http://dx.doi.org/10.1056/NEJM198902163200701

62. Meehan J, Piano MR, Solaro RJ, Kennedy JM. Heavy long-term ethanol consumption induces an alpha- to beta-myosin heavy chain isoform transition in rat. Basic Res Cardiol [Internet]. 1999 Dec;94(6):481–8 PMID10651160. Available from: http://dx.doi.org/10.1007/s003950050164

63. Hunter RJ, Neagoe C, Järveläinen HA, Martin CR, Lindros KO, Linke WA, et al. Alcohol affects the skeletal muscle proteins, titin and nebulin in male and female rats. J Nutr [Internet]. 2003 Apr 1 [cited 2022 Jul 11];133(4):1154–7. Available from: https://academic.oup.com/jn/article/133/4/1154/4688261

64. David P, Subramaniam K. Prenatal alcohol exposure and early postnatal changes in the developing nerve-muscle system. Birth Defects Res A Clin Mol Teratol [Internet]. 2005 Nov;73(11):897–903 PMID16228975. Available from: http://dx.doi.org/10.1002/bdra.20190

65. Myrie SB, Pinder MA. Skeletal muscle and fetal alcohol spectrum disorder. Biochem Cell Biol [Internet]. 2018 Apr;96(2):222–9 PMID29091741. Available from: http://dx.doi.org/10.1139/bcb-2017-0118

66. Davis TA, Fiorotto ML. Regulation of muscle growth in neonates. Curr Opin Clin Nutr Metab Care [Internet]. 2009 Jan;12(1):78–85 PMID19057192PMC2653196. Available from: http://dx.doi.org/10.1097/MCO.0b013e32831cef9f

67. Lin G, Wang X, Wu G, Feng C, Zhou H, Li D, et al. Improving amino acid nutrition to prevent intrauterine growth restriction in mammals. Amino Acids [Internet]. 2014 Jul;46(7):1605–23 PMID24658999. Available from: http://dx.doi.org/10.1007/s00726-014-1725-z

68. Olney JW, Wozniak DF, Jevtovic-Todorovic V, Farber NB, Bittigau P, Ikonomidou C. Glutamate and GABA receptor dysfunction in the fetal alcohol syndrome. Neurotox Res [Internet]. 2002 Jun;4(4):315–25 PMID12829421. Available from: http://dx.doi.org/10.1080/1029842021000010875

69. Davies M. The role of GABAA receptors in mediating the effects of alcohol in the central nervous system. J Psychiatry Neurosci [Internet]. 2003 Jul;28(4):263–74 PMID12921221PMC165791. Available from: https://www.ncbi.nlm.nih.gov/pubmed/12921221

70. Lobo IA, Harris RA. GABA(A) receptors and alcohol. Pharmacol Biochem Behav [Internet]. 2008 Jul;90(1):90–4 PMID18423561PMC2574824. Available from: http://dx.doi.org/10.1016/j.pbb.2008.03.006

71. Smiley JF, Saito M, Bleiwas C, Masiello K, Ardekani B, Guilfoyle DN, et al. Selective reduction of cerebral cortex GABA neurons in a late gestation model of fetal alcohol spectrum disorder. Alcohol [Internet]. 2015 Sep;49(6):571–80 PMID26252988PMC4554880. Available from: http://dx.doi.org/10.1016/j.alcohol.2015.04.008

72. Wozniak JR, Fink BA, Fuglestad AJ, Eckerle JK, Boys CJ, Sandness KE, et al. Four-year follow-up of a randomized controlled trial of choline for neurodevelopment in fetal alcohol spectrum disorder. J Neurodev Disord [Internet]. 2020 Mar 12;12(1):9 PMID32164522PMC7066854. Available from: http://dx.doi.org/10.1186/s11689-020-09312-7

837 73. Milbocker KA, Klintsova AY. Examination of cortically projecting cholinergic neurons
838 following exercise and environmental intervention in a rodent model of fetal alcohol
839 spectrum disorders. Birth Defects Res [Internet]. 2021 Feb 1;113(3):299–313
840 PMID33174398PMC8274426. Available from: http://dx.doi.org/10.1002/bdr2.1839

841 74. Macht VA, Vetreno RP, Crews FT. Cholinergic and neuroimmune signaling interact
842 to impact adult hippocampal neurogenesis and alcohol pathology across
843 development. Front Pharmacol [Internet]. 2022 Mar 2;13:849997
844 PMID35308225PMC8926387. Available from:
845 http://dx.doi.org/10.3389/fphar.2022.849997

846 75. Hawkins EG, Martin I, Kondo LM, Judy ME, Brings VE, Chan C-L, et al. A novel
847 cholinergic action of alcohol and the development of tolerance to that effect in
848 Caenorhabditis elegans. Genetics [Internet]. 2015 Jan;199(1):135–49
849 PMID25342716PMC4286678. Available from:
850 http://dx.doi.org/10.1534/genetics.114.171884

851 76. Kaufman MH. Ethanol-induced chromosomal abnormalities at conception. Nature
852 [Internet]. 1983; PMID6682181. Available from: http://dx.doi.org/10.1038/302258a0

853 77. Kaufman MH, Bain IM. Influence of ethanol on chromosome segregation during the
854 first and second meiotic divisions in the mouse egg. J Exp Zool [Internet]. 1984;
855 PMID6429271. Available from: http://dx.doi.org/10.1002/jez.1402300217

856 78. Shi Q, Martin RH. Aneuploidy in human sperm: a review of the frequency and
857 distribution of aneuploidy, effects of donor age and lifestyle factors. Cytogenet Cell
858 Genet [Internet]. 2000;90(3–4):219–26 PMID11124518. Available from:
859 http://dx.doi.org/56773

860 79. Mews P, Egervari G, Nativio R, Sidoli S, Donahue G, Lombroso SI, et al. Alcohol
861 metabolism contributes to brain histone acetylation. Nature [Internet].
862 2019;574(7780):717–21 PMID31645761. Available from:
863 http://dx.doi.org/10.1038/s41586-019-1700-7

Table 1

Pathway	Generation/Condition
Peptide metabolic process	F105,F305,F1005,F3005
Carboxylic acid metabolic process	F105,F305,F1005,F3005
Small molecule biosynthetic process	F105,F305,F1005,F3005
Defense response	F105,F305,F1005,F3005
Translation	F105,F305,F1005
Embryo development ending in birth or egg hatching	F105,F305,F1005
Aging	F105,F1005,F3005
Ribosomal large subunit biogenesis	F105,F305,F1005
Ribosome assembly	F105,F305,F1005
Cytoskeleton organization	F105,F305,F3005
Multi-organism process	F105,F305,F1005
Ribose phosphate metabolic process	F105,F305,F1005
Cellular process involved in reproduction in multicellular organism	F105,F305,F1005
Actin cytoskeleton organization	F105,F305,F3005
Protein catabolic process	F105,F1005,F3005
Response to heat	F105,F305,F1005
Multicellular organismal movement	F105,F305,F3005
rRNA binding	F105,F305,F1005
Phosphotransferase activity, phosphate group as acceptor	F105,F305,F1005
Threonine-type endopeptidase activity	F105,F305,F1005

Table 1: Shared pathways identified through DEG analysis across both exposures and generations.

Top 20 shared pathways identified by the union of all cell type specific DEGs across the four conditions. F105 indicates 0.5% ethanol exposure at the F1 generation. F1005 indicates 0.05% ethanol exposure at the F1 generation. F305 indicates 0.5% ethanol exposure at the F3 generation. F3005 indicates 0.05% ethanol exposure at the F3 generation.

873 **Figure 1: Adult *C. elegans* snRNA-seq sample preparation, analysis, and t-SNE**
874 **projection**

875 **A.** Experimental flow for single-nucleus isolation and snRNA-seq analysis. **B.** t-
876 distributed stochastic neighbor embedding (t-SNE) plot of cells from all the samples with
877 clustering through unsupervised Louvain clustering. Cluster molecular characterization
878 and identity is presented in the corresponding dashboard (Supplemental file 1).

879

880 **Figure 2: Cluster-resolved expression of cell type-specific markers.**

881 Example of cluster-specific expression of cell type specific markers for the
882 spermatheca, epithelial cells, GABA and mechanosensory neurons, germline, and
883 coelomocyte. Right column: cluster specific expression. Middle column: representative
884 *in situ* expression data from NEXTDB for corresponding marker. Left column: gene
885 expression dot plot of known cell type specific markers.

886

887 **Figure 3: Global and cluster-specific alterations in gene expression by inter- or**
888 **trans-generational ethanol exposure.**

889 **A.** Venn diagram based on the union of DEGs across all the cell types, separated by
890 Up-regulated DEGs only (left), Downregulated genes only (right), and all DEGs
891 (middle). **B, C.** Euclidean distance sensitivity analysis of all the cell clusters at the F1
892 generation (B) or F3 generation (C). X-axis indicates cluster number and y-axis
893 indicates log fold change compared to Euclidean distance obtained by permuting
894 treatment labels. Significance was assessed based on comparing Euclidean distance
895 against 1,000 random permutated labels. **D, E.** Expression of *tra-2* in cluster 23 at the

F1 (D) and *mex-3* in cluster 12 at the F3 (E). **F-I.** Validation of snRNA-seq data through single molecule fluorescence *in situ* hybridization (smFISH) by confocal imaging (F,G) followed by FISH-Quant (H,I). Scale bar 5 µm. 3 biological replicates, 2 worms per repeat, 10 nuclei per germline. *P<0.05, ***P<0.001. Welch's t-test.

Figure 4: Phenotypic enrichment in response to inter- or trans-generational ethanol exposure.

A,C. Dot heatmap of top shared WormBase phenotype across cell types with significantly altered Euclidean distance metric at the F1 (A) or F3 (C). Dot size corresponded to -log(FDR) obtained from enrichment analysis and dot color corresponded -log(median fold change) of overlapping genes in each pathway. **B,D**. Bar plot showing the proportion of top WormBase phenotype annotations from all enriched pathways ("dataset") and WormBase phenotype database ("Background_all_path") at the F1 (B) or F3 (D). For each WormBase phenotype from the original database we retrieved the corresponding WormBase phenotype annotations by querying EBI OLS API, followed by selecting the top 20 shared phenotypes. Proportions were calculated based on the proportion of annotations among all enriched pathways ("dataset") and the WormBase phenotype database ("Background_all_path"). Fisher's exact test was used to compare proportions between the two conditions in each annotation category.

Figure 5: P0 ethanol exposure causes reproductive dysfunction at the F1 and F3 generations.

P0 hermaphrodites were exposed to water, 0.05% ethanol, or 0.50% ethanol. **A,B.** Number of apoptotic nuclei per gonadal arm in N2 worms at the F1 and F3 exposed to the indicated ethanol levels, N=4-5, 22 worms per repeat. Scale bars = 10µm. **C.** Assessment of errors of X chromosome segregation as measured by *Pxol-1::gfp* reporter. Out of 30 total worms per repeat, the percent (%) of worms with at least 1 GFP+ embryo was recorded, N=6, 30 worms per repeat. **D.** Percent embryonic lethality per worm was measured for N2, N=4-10, 2-3 worms per repeat (D). One-way ANOVA with Dunnet correction. *P<0.05, **P<0.01, ***P<0.001, ****P<0.0001.

Figure 1

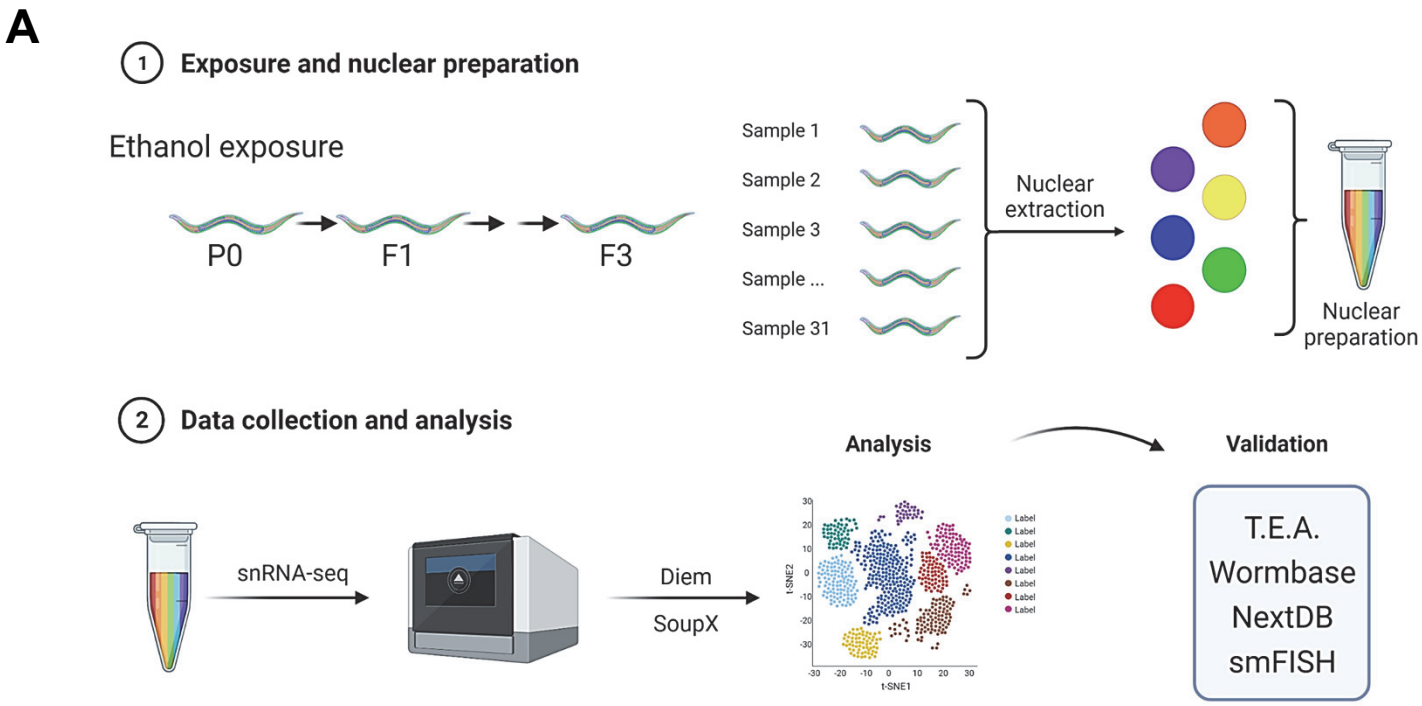

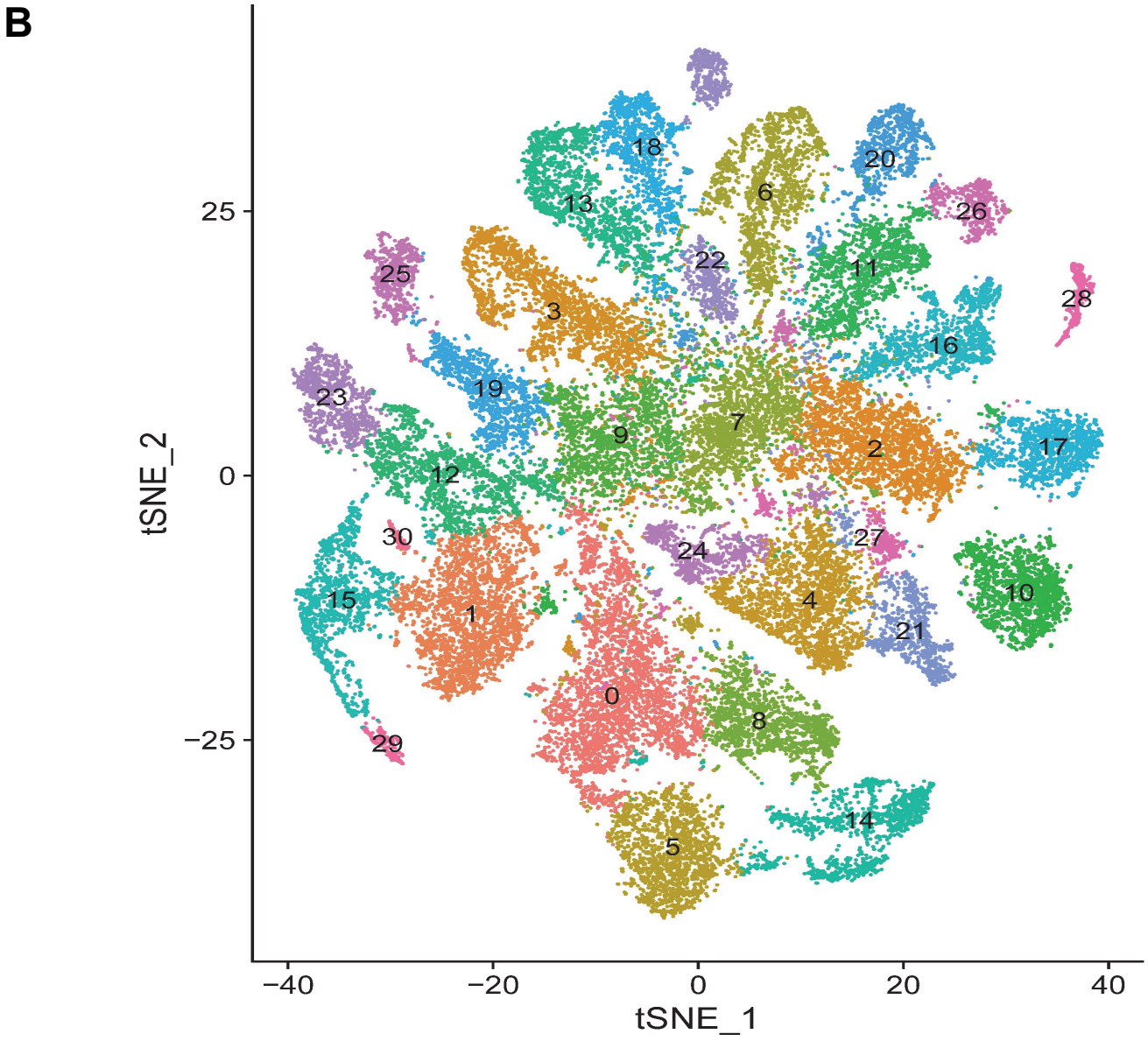

Figure 2

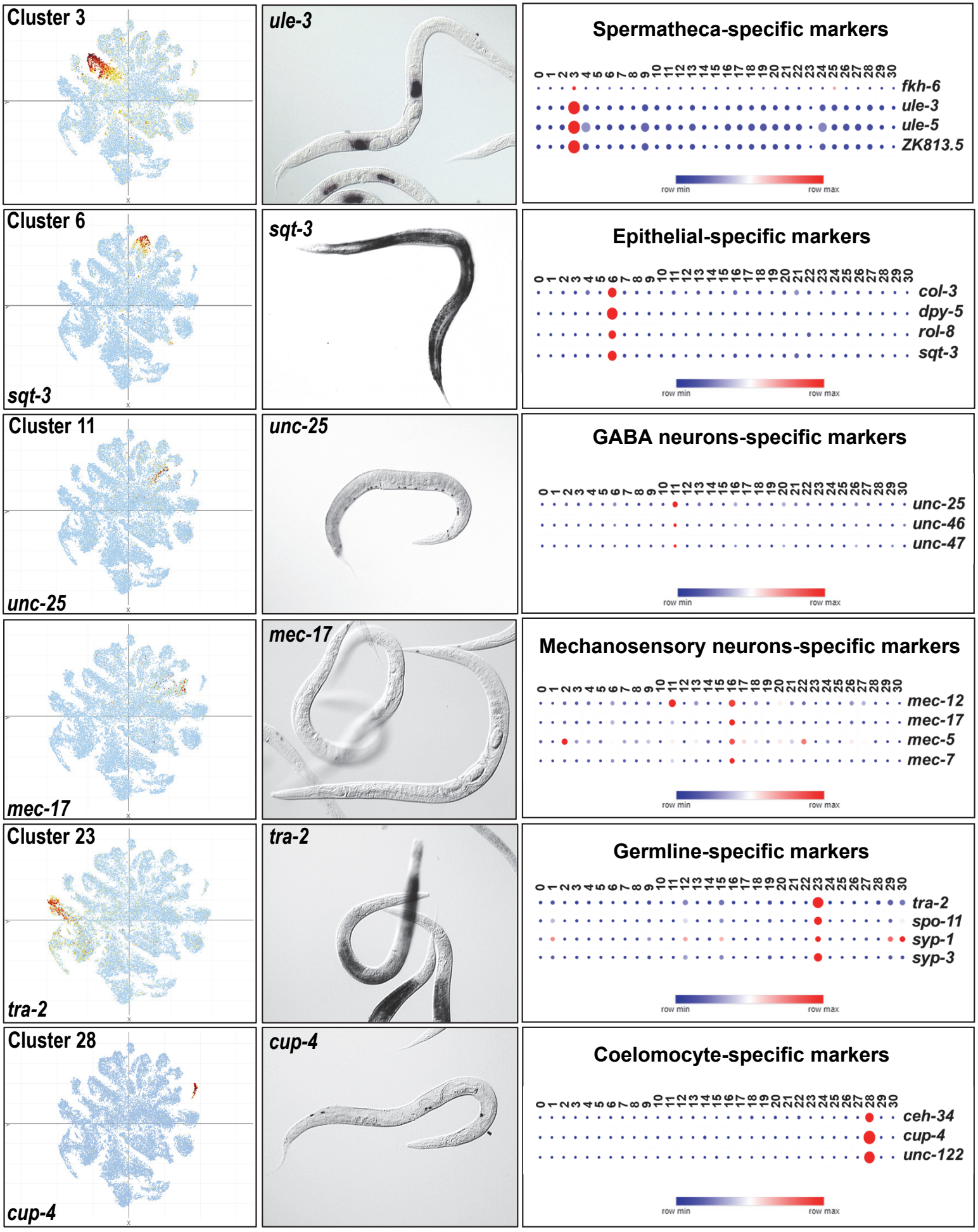

Figure 3

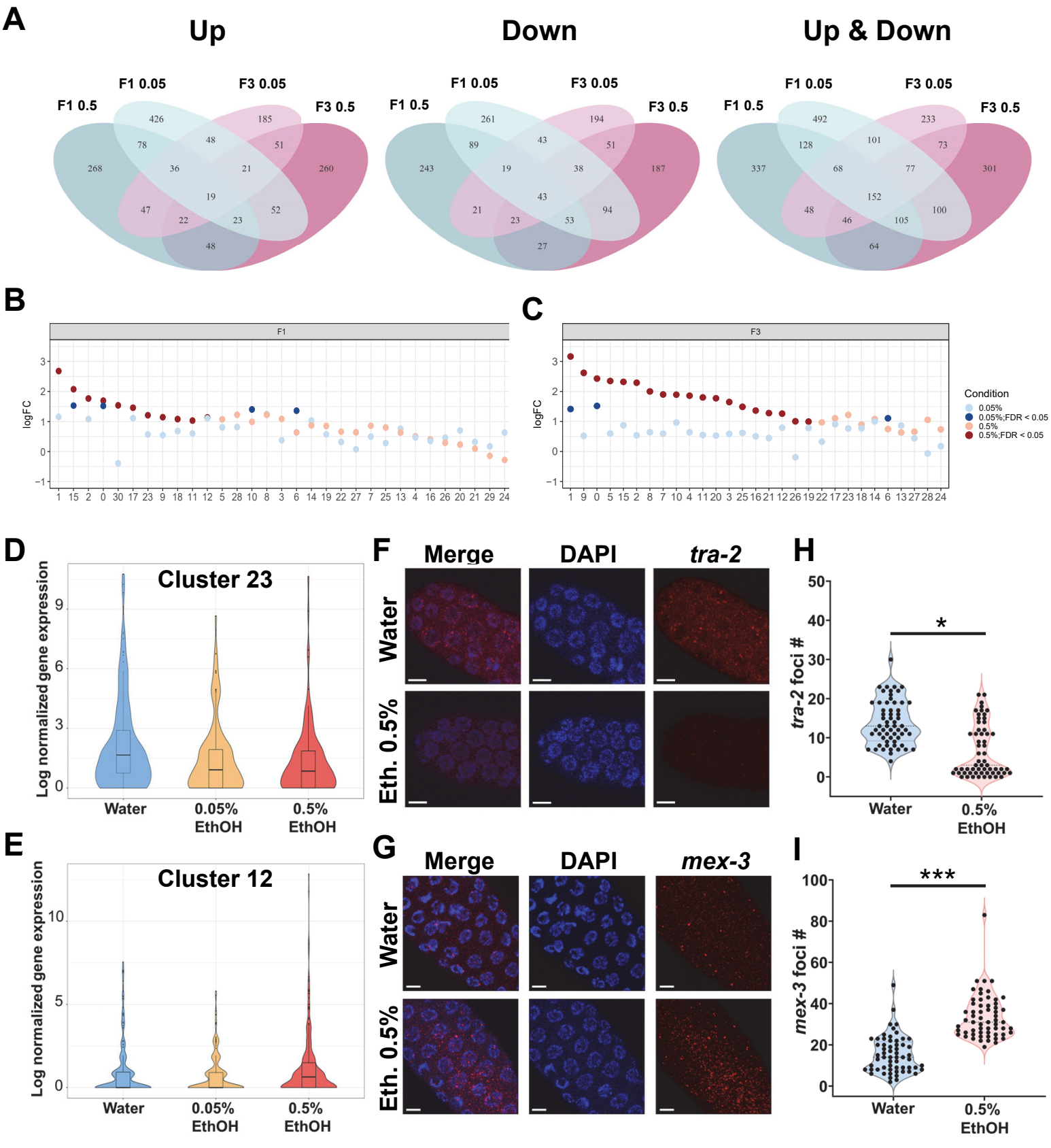

Figure 4

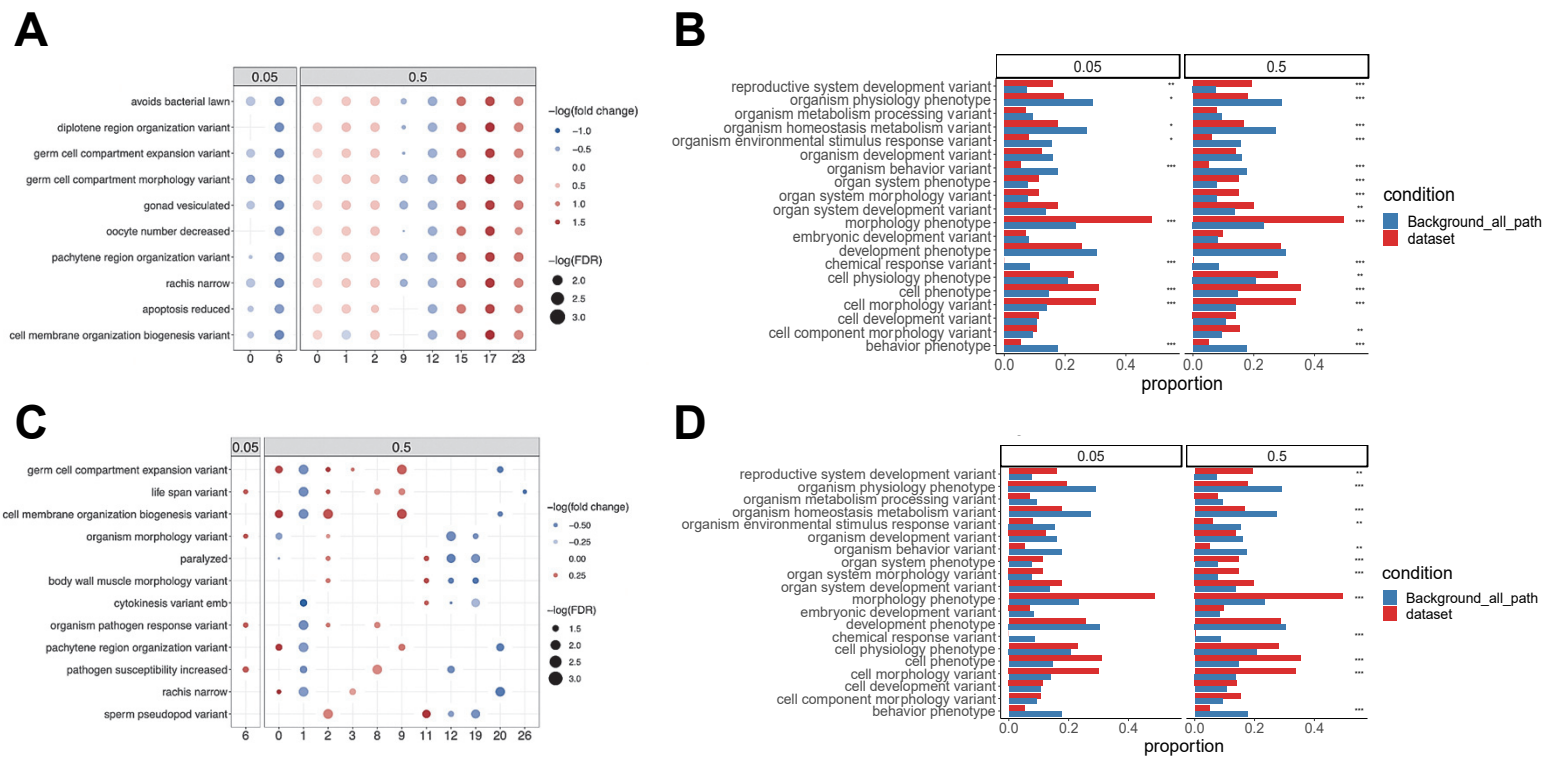

Figure 5

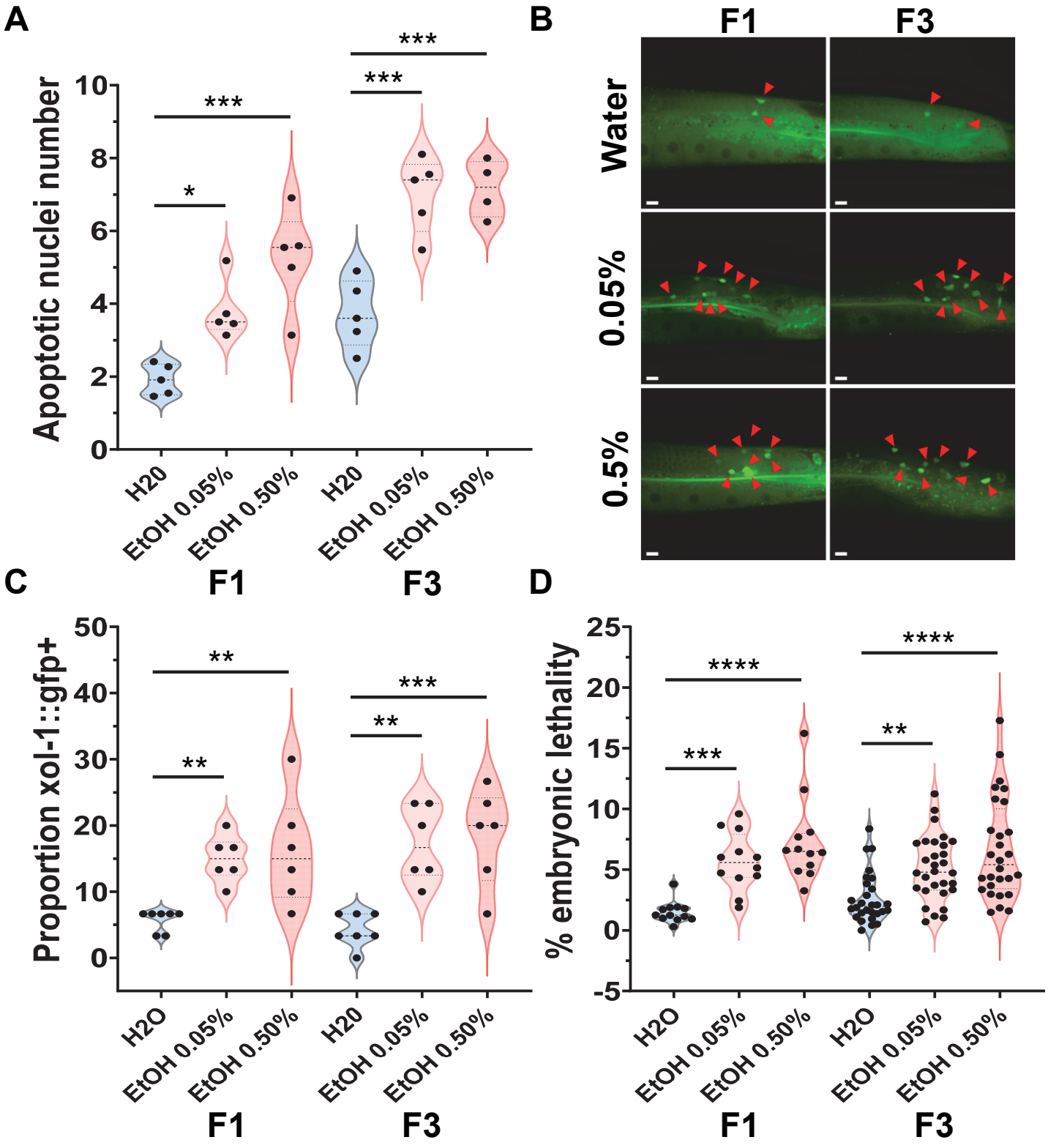

Figure S1

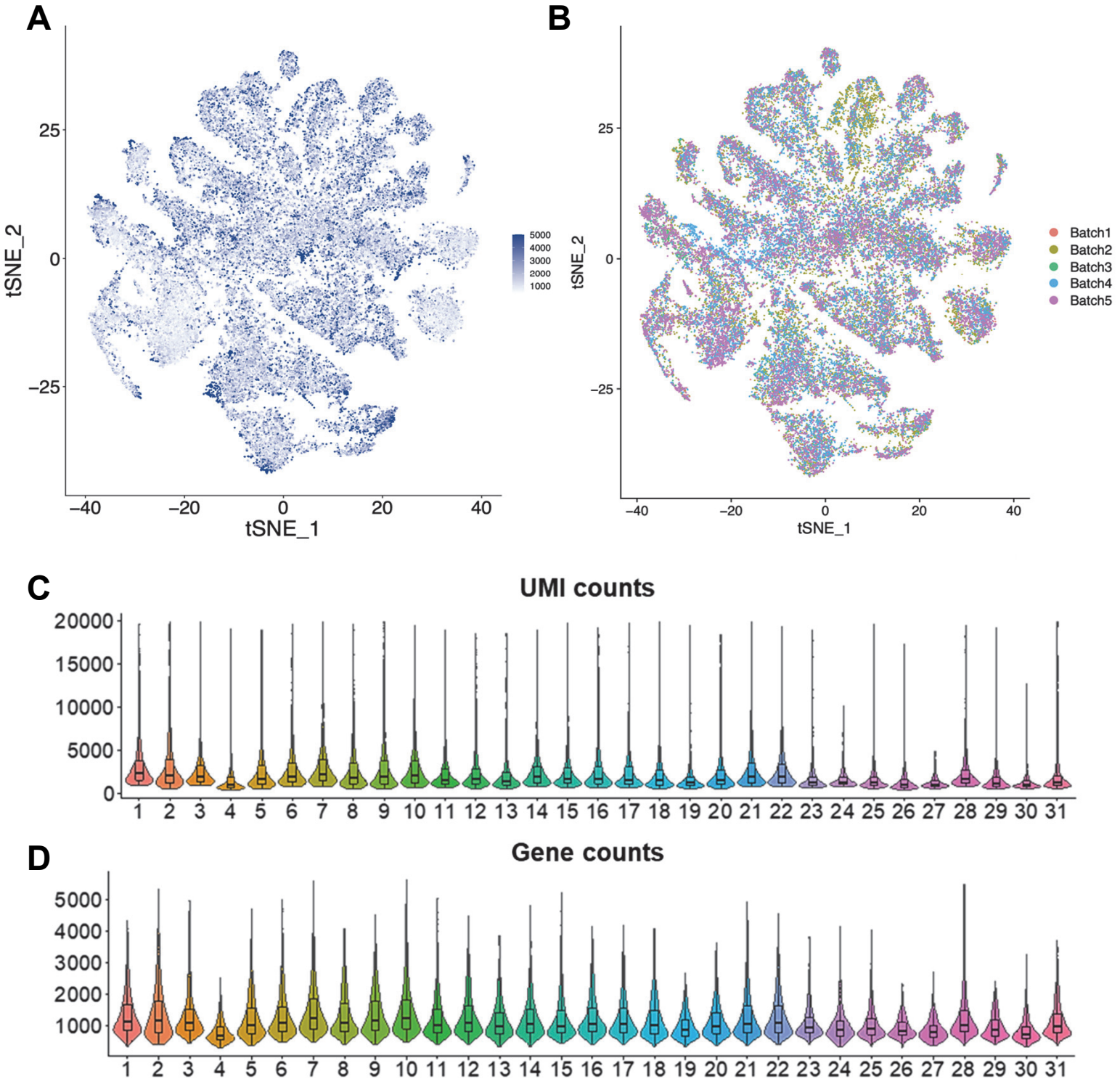

Figure 1: UMI, gene count, and batch distributions

A. UMI (unique molecular identifier) distribution as tSNE plot. X and Y-axis are representative tSNE axis. Each dot represents a cell and color scale Is plotted based on UMI count in each cell. UMI lower than 1000 are plotted as 1000 and higher than 5000 are plotted as 5000. **B,** tSNE plot colored by batch after batch effect correction by canonical correlation analysis. **C,D.** Violin and boxplot of UMI (unique molecular identifier) and gene counts per cell in each sample across 31 single-nuclei samples.

Figure S2

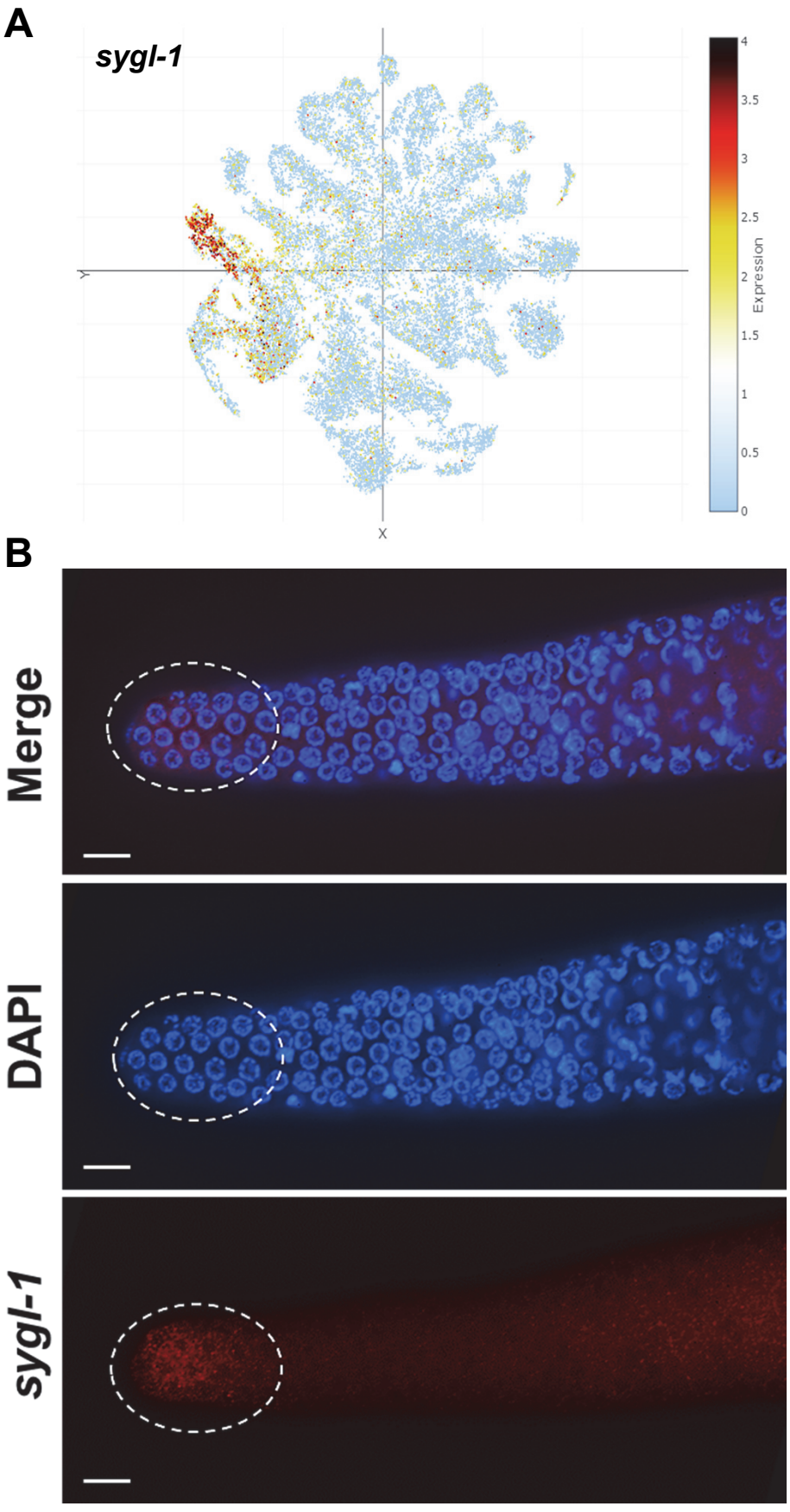

Figure S2: tSNE expression and smFISH for *sygl-1* transcript
A. Expression of *sygl-1* transcript from the adult *C. elegans* snRNA-seq data set. The bulk of its expression resolves to cluster 23. **B.** smFISH for *sygl-1* transcript showing its well-described expression within the distal gonad (circle) as well as some expression more proximally. Scale bar = 10μm.

Figure S3

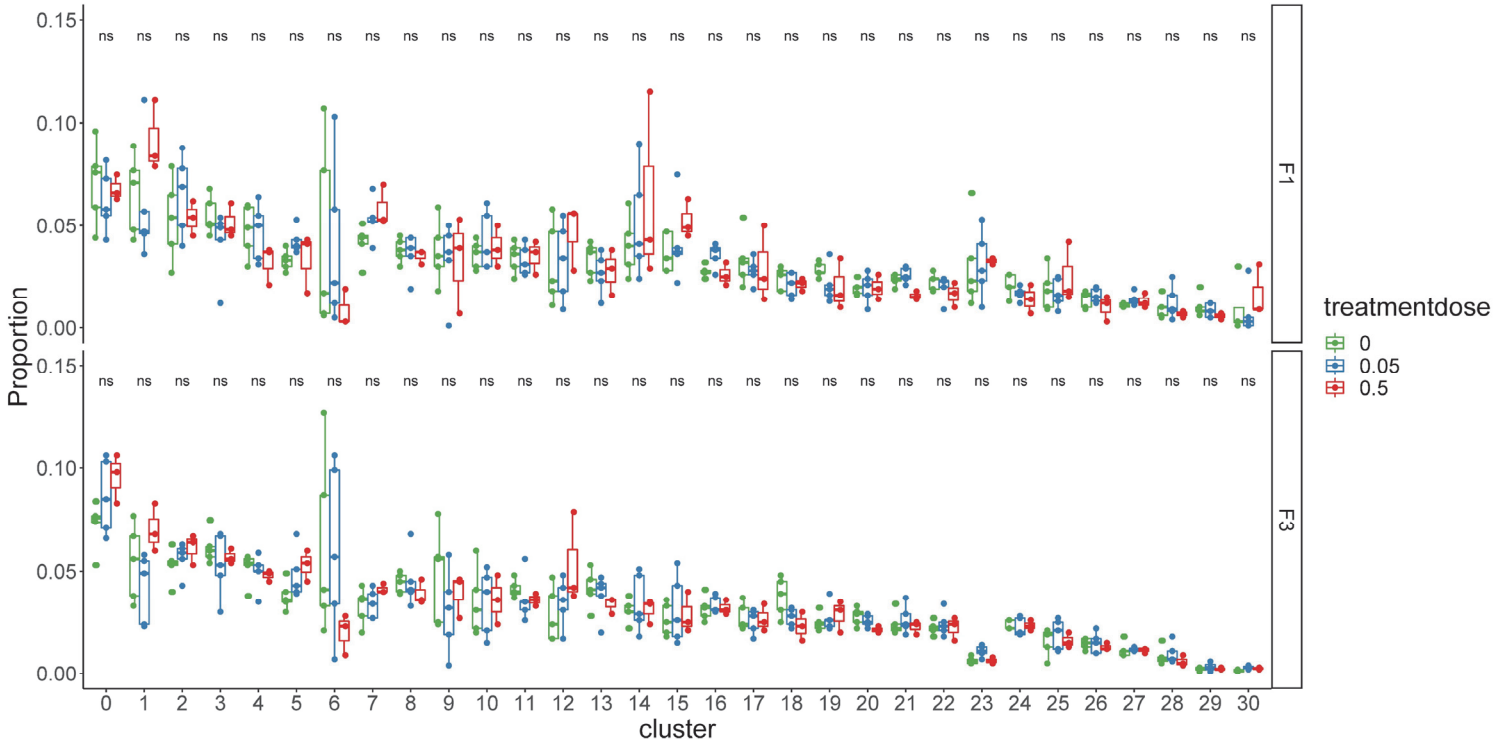

Figure S3: F1 and F3 cluster proportions

Proportion distribution plot of all F1 and F3 samples colored by different treatment dose (0, 0.05%, and 0.5% ethanol), each dot represents one sample. X-axis indicates cluster number assigned by Louvain clustering and Y-axis indicates cells of that cluster divided by all cells from that specific sample. All conditions were non-significant based on post-hoc Tukey statistic.

Figure S4

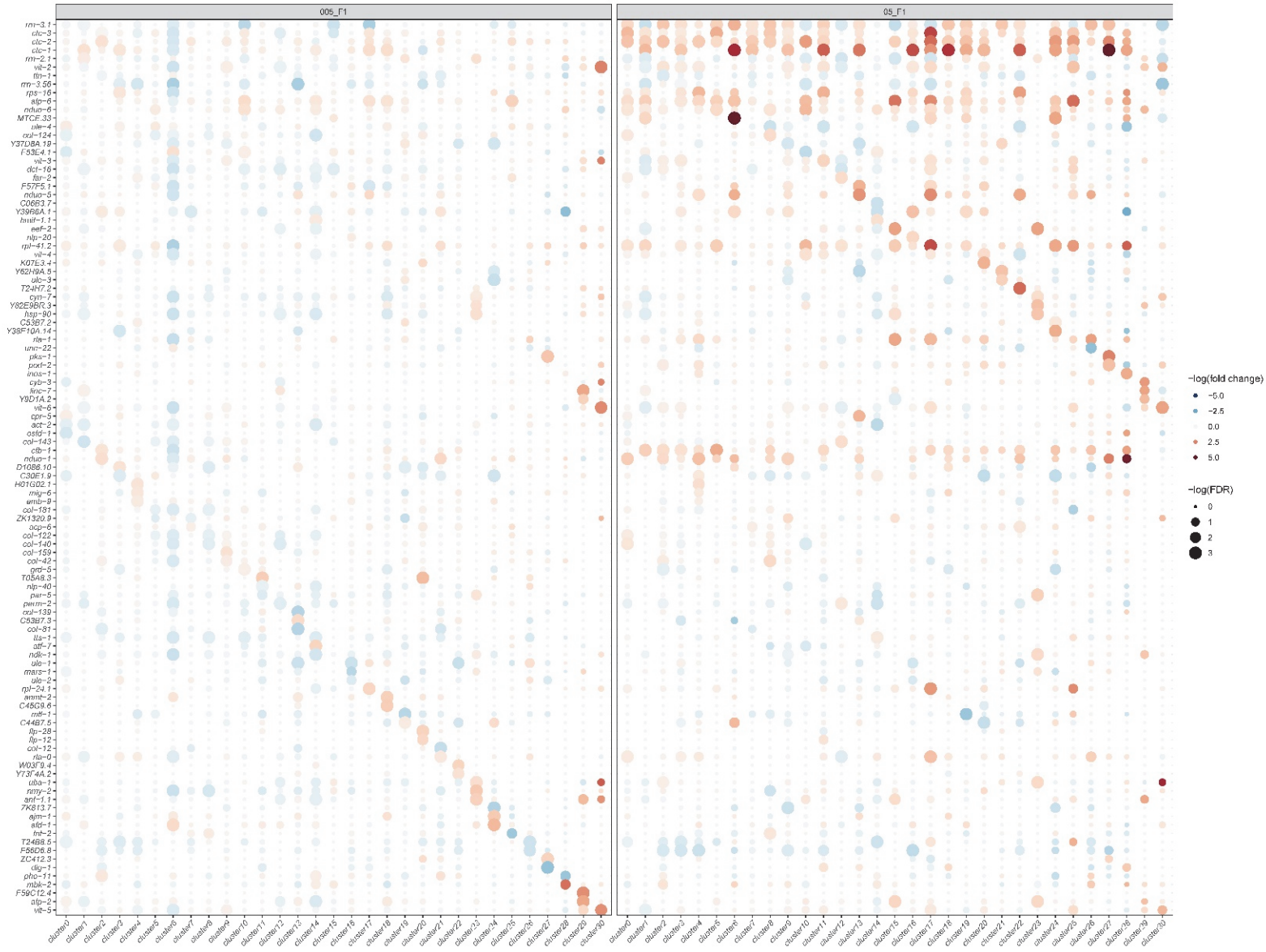

Figure S4: Dot heatmap of top 3 differential expressed genes across clusters at the F1. X-axis indicates different clusters representing different tissues and Y-axis indicates top 3 differentially expressed genes after ethanol treatment across clusters ranked by monocle based FDR. The plot is further separated by different ethanol doses (0.05% on the left and 0.5% on the right). The size of the dot is correlated to –log(FDR) of differential expression p-value and the color represents direction and scale of fold change with upregulation is shown in red and downregulation is shown in blue.

Figure S5

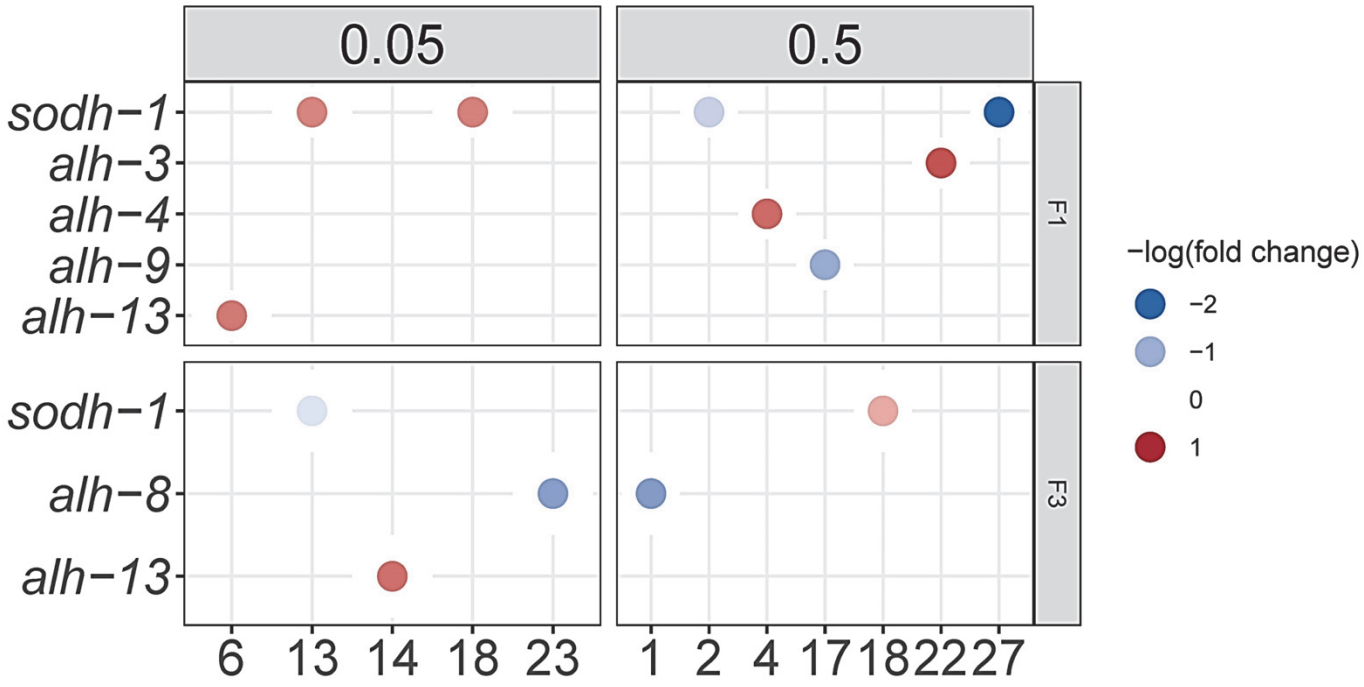

Figure S5: Cluster-specific DEGs related to ethanol metabolism at F1 and F3.
Dot heatmap of ethanol metabolism related genes across different clusters, separated by exposure dose (0.05% or 0.5% ethanol) and generation (F1 or F3). Only DEGs with an FDR < 5% were plotted. Color indicates –log10(fold change).

Figure S6

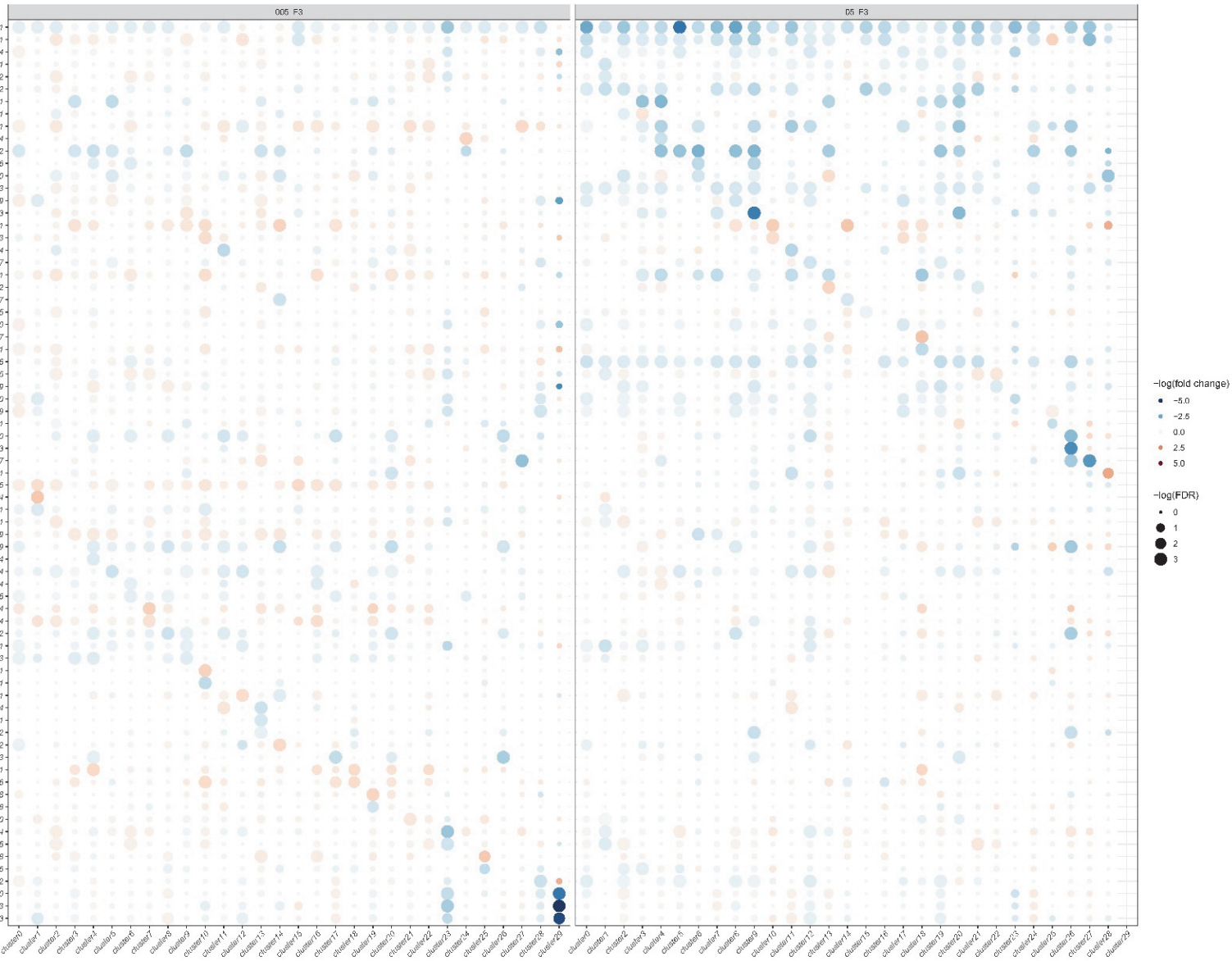

Figure S6: Dot heatmap of top 3 differential expressed genes across clusters at the F3.

X-axis indicates different clusters representing different tissues and Y-axis indicates the top 3 differentially expressed genes after ethanol treatment across clusters ranked by monocle based FDR. The plot is further separated by different ethanol doses (0.05% on the left and 0.5% on the right). The size of the dot is correlated to –log(FDR) of differential expression p-value and the color represents direction and scale of fold change with upregulation is shown in red and downregulation is shown in blue.